AD-A234 526

RADC-TR-90-220
Final Technical Report
October 1990
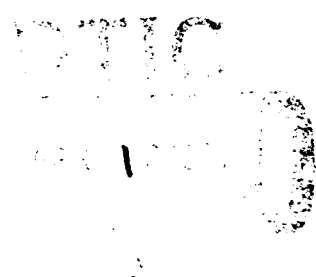
STUDY OF JOSEPHSON EFFECT ARRAYS AS SOURCES AT 1 THZ

State University of New York (SUNY)

Sponsored by
Strategic Defense Initiative Office

APPROVED FOR PUBLIC RELEASE; DISTRIBUTION UNLIMITED.

The views and conclusions contained in this document are those of the authors and should not be interpreted as necessarily representing the official policies, either expressed or implied, of the Strategic Defense Initiative Office or the U.S. Government.
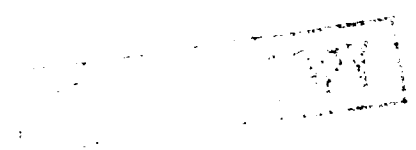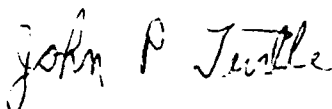
**Rome Air Development Center
Air Force Systems Command
Griffiss Air Force Base, NY 13441-5700**

This report has been reviewed by the RADC Public Affairs Division (PA) and is releasable to the National Technical Information Service (NTIS). At NTIS it will be releasable to the general public, including foreign nations.

RADC-TR-90-220 has been reveiwed and is approved for publication.

APPROVED: *John P Turtle*
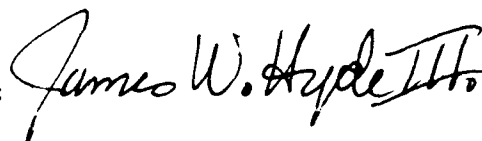
JOHN P. TURTLE
Project Engineer

APPROVED: *John K. Schindler*

JOHN K. SCHINDLER
Director of Electromagnetics

FOR THE COMMANDER: *James W. Hyde III*

JAMES W. HYDE III
Directorate of Plans & Programs

STUDY OF JOSEPHSON EFFECT ARRAYS AS SOURCES AT 1 THZ

James Lukens

REPORT DOCUMENTATION PAGE

Form Approved
OMB No. 0704-0188

Public reporting burden for this collection of information is estimated to average 1 hour per response, including the time for reviewing instructions, searching existing data sources, gathering and maintaining the data needed, and completing and reviewing the collection of information. Send comments regarding this burden estimate or any other aspect of this collection of information, including suggestions for reducing this burden, to Washington Headquarters Services, Directorate for Information Operations and Reports, 1215 Jefferson Davis Highway, Suite 1204, Arlington, VA 22202-4302, and to the Office of Management and Budget, Paperwork Reduction Project (0704-0188), Washington, DC 20503.

1. AGENCY USE ONLY (Leave Blank)	2. REPORT DATE October 1990	3. REPORT TYPE AND DATES COVERED Final Aug 86 - Jan 90

4. TITLE AND SUBTITLE
STUDY OF JOSEPHSON EFFECT ARRAYS AS SOURCES NEAR 1 THz

5. FUNDING NUMBERS
C - F19628-86-K-0039
PE - 63221C
PR - S812
TA - C1
WU - 23

6. AUTHOR(S)
James Lukens

7. PERFORMING ORGANIZATION NAME(S) AND ADDRESS(ES)
State University of New York (SUNY)
Department of Physics
Stony Brook NY 11794

8. PERFORMING ORGANIZATION REPORT NUMBER

9. SPONSORING/MONITORING AGENCY NAME(S) AND ADDRESS(ES)
Strategic Defense Initiative Office, Office of the Secretary of Defense Wash DC 20301-7100

Rome Air Development Center (EEAA) Hanscom AFB MA 01731-5000

10. SPONSORING/MONITORING AGENCY REPORT NUMBER
RADC-TR-90-220

11. SUPPLEMENTARY NOTES
RADC Project Engineer: John P. Turtle/EEAA/(617) 377-2051

12a. DISTRIBUTION/AVAILABILITY STATEMENT
Approved for public release; distribution unlimited.

12b. DISTRIBUTION CODE

13. ABSTRACT (Maximum 200 words)

Techniques have been developed and tested for coupling 40 junction arrays of Josephson effect oscillators to achieve coherent operation in the submillimeter wave range. Arrays have been fabricated using both lead alloy and niobium trilayer technology. Coherent operation has been demonstrated between 150 GHz and 500 HGz. The maximum power was developed at 400 GHz where 7 microwatts was delivered to a 20 Ohm on-chip load.

14. SUBJECT TERMS
Superconductor, Submillimeter Wave Source, Josephson Effect Source, Coherent Arrays

15. NUMBER OF PAGES
69

16. PRICE CODE

17. SECURITY CLASSIFICATION OF REPORT UNCLASSIFIED	18. SECURITY CLASSIFICATION OF THIS PAGE UNCLASSIFIED	19. SECURITY CLASSIFICATION OF ABSTRACT UNCLASSIFIED	20. LIMITATION OF ABSTRACT UL

NSN 7540-01-280-5500

Standard Form 298 (Rev 2-89)
Prescribed by ANSI Std Z39-18
298-102

I.   Final report summary

a) Task objectives: The major objectives of this contract were the development and demonstration of submillimeter wave sources based on arrays of Josephson junction oscillators.

b) Technical problems: The main technical problem in this effort was the development of a method for coherently phase locking large arrays of Josephson junction oscillators spread over many wavelengths. Additionally numerous techniques had to be developed to fabricate these array sources using niobium trilayer technology. A particular problem was the need to develop a new method for the fabrication of very low inductance (sub-picohenry) shunt resistors for junctions made using this technology.

c) General methodology: Various array structures were analyzed using perturbation techniques discussed in Appendix A, Sections 4 and 5, in order to develop an appropriate array design. Test chips incorporating these designs were fabricated and tested at temperatures between 1.5 and 4.2 K. The power generated by the arrays was measured as a function of frequency between 100 GHz and 500 GHz. Improved designs were developed based on these measurements.

d) Technical results: The main technical results are presented in Appendix A, Section 6. These include the generation and coupling of 7 μW of power to a 20 Ω load at a frequency of 400 GHz. This was a new record for an IC source operating at its fundamental frequency. Single sources have generated significant power levels (of order of a microwatt) over the range of 150 GHz to 450 GHz.

e) Important findings and conclusions: It has been demonstrated that distributed arrays of Josephson junction oscillators can be coherently coupled to efficiently deliver power to high impedance loads in the submillimeter wave range. Larger arrays based on the concepts developed should generate 0.1 mW of power. It was shown that suitable junctions with resistive shunts could be made using the robust niobium technology. Arrays using niobium transmission lines should operate to about 700 GHz, limited by the

losses in the lines. Using a higher T_c material, e.g., NbN for the transmission lines but continuing to use Nb junctions, should increase the upper limit to about 1.5 THz.

f) Implications for further research: Our results have suggested methods to extend both the frequency and power of array sources. These techniques, which are discussed in more detail in Appendix A, Section 7, include the use of high T_c materials and of arrays using wide junction and/or having a two-dimensional distribution of junctions in contrast to the one-dimensional arrays studied under the present contract.

g) Significant hardware development: The main hardware developed as part of this contract was the 40 junction array IC discussed above and in more detail in Section 6 of Appendix A.

II.   Scientists and engineers contributing to report

Dr. Aloke K. Jain

Mr. Joseph Montani

Mr. Yi Liu

Mr. Kelin Wan

Mr. To Chi Leung

Mr. Baokang Bi

Mr. Lan Vu

Mr. Linus Fetter

Professor James Lukens

III.   Publications resulting from work supported under this contract

"Josephson Arrays as High Frequency Sources"
James Lukens
Chapter in *Modern Superconducting Devices*, S. Ruggiero and D. Rudman, Eds., Academic Press, Boston, 1990.

"Submillimeter Wave Generation Using Josephson Junction Arrays"
K. Wan, A.K. Jain, J.E. Lukens
Appl. Phys. Lett. 63, 1805 – 1807 (1989)

"Submillimeter Wave Generation Using Josephson Junction Arrays"
K-L. Wan, A.K. Jain, J.E. Lukens
IEEE Trans. Magn., MAG-25, 1076-1079 (1989)

"Application of Josephson Effect Arrays for Submillimeter Sources"
J.E. Lukens, A.K. Jain, and K.L. Wan
Superconducting Electronics, H. Weinstock and M. Nisenoff, Eds. NATO ASI Series
(Proceedings of the NATO Advanced Study Institute on Superconducting Electronics, held
in Il Ciocco, Italy, June 26 – July 8, 1988), Series F: Computer and Systems Sciences Vol.
59 , Springer-Verlag, 1989.

"Using the Josephson Effect for Millimeter and Submillimeter Wave Generation"
J. Sauvageau, A.K. Jain, J.E. Lukens
*Sensing, Discrimination, and Signal Processing and Superconducting Materials and
Instrumentation*, Roy Nichols, James A. Ionson, Eds., Proc. SPIE 879, 69-70 (1988)

"Phase-locking in Distributed Arrays of Josephson Oscillators"
J.E. Sauvageau, A.K. Jain, J.E. Lukens, R.H. Ono
IEEE Trans. Magn., MAG-23, No. 2, 1048-1050 (1987)

IV.   Recapitulation of periodic reports

The major effort during the first period was the acquisition and and initial

construction of equipment needed for this research. We worked to develop a new electron

beam lithography system to permit writing of arrays over large areas of a wafer. Work

also began to test the performance of our Josephson junctions at frequencies up to 1 THz.

These areas would be the focus of work during the coming three month period.

During the second period the scanning electron microscope and other components

arrived for the new EBL (electron beam lithography) system which we would be building

and which would be crucial for the large arrays to be fabricated during the later stages of

this project. Work began to interface the beam control electronics to a comuter for

pattern generation. Work also began on building the laser interferometer controlled stage

for positioning the wafers during beam writing. Measurements were made to test the

performance of our resistively shunted lead alloy junctions at high frequencies. Data

indicated that their performance was essentially ideal up to at least 600 GHz. This was

near the useful upper limit of lead due to excessive transmission line losses at high

frequencies. We thus concluded, as anticipated, that the lead alloy technology would be

adequate for the first phase of the project. For operation above one terahertz, refractory metals, e.g. NbN, would be required. In anticipation of this, work was begun to construct a plasma etching system required for patterning the Nb films.

In period three the development work proceeded as expected. In particular the beam control hardware for our new, large field EBL system was nearly finished, and work continued to develop NbAℓNb trilayers for later use in high frequency circuits. The results of our AFOSR-sponsored project to test concepts for a 100 GHz Josephson array source demonstrated that the design for phase-locking the junctions in distributed arrays, which we planned to use for the THz sources, performed as expected. However, as a result of that work we concluded that the junction uniformity required for a fully phase-locked array implied a critical current spread with a standard deviation of less than about 1% -- about half that expected when we began the work. A potential solution to this problem, which would avoid the necessity to upgrade our present junction fabrication process, was to current bias the junctions in parallel instead of in series. In this way the bias currents automatically divide up so as to compensate, to first order, for the nonuniformity in junction critical currents. One drawback to this approach was that it was necessary to carefully filter the many bias leads to the array in order to avoid perturbing its rf properties. Our first tests of this new design were encouraging in that the power increased by a factor of ten over that from a similar series biased array, giving $0.04\mu W$ at 300 GHz. This first attempt had rather crude rf filters on the bias leads. We expected that this poor filtering was the reason that the theoretical power of $0.1\mu W$ was not achieved and started work to refine the design of these filters.

Our major result during the fourth period was to obtain power levels of about $1\mu W$ from Josephson effect arrays operating near 300 GHz. The "breakthrough" which led to these results was the parallel biasing scheme previously reported. In that array the junction spacing was 1mm, the wavelength at 100 GHz. Since this array preferred to operate at 300 GHz, presumably because of the load impedance seen by the junctions, we

5

reduced the junction spacing by a factor of 3 to give a fundamental operating frequency of 300 GHz. This, along with some refinements in coupling the bias leads to the array, resulted in a series of three arrays with power levels of 0 2μW, 0.4μW, and 0.8μW. The $I_c R$ product of the junctions used in these arrays corresponded to a frequency of 75 GHz, far below the operating frequency. This was caused by the relatively low critical current of about 300μA. Since power would increase as I_c^2 under these conditions, the prospect existed for a substantial power increase just by increasing I_c.

Our primary effort during the fifth period was to conduct a series of systematic measurements on the parallel biased arrays from which we had been obtaining 1μW of power at 350 GHz. For example, we were measuring properties of the individual junctions comprising the array in order to more accurately compare our results with theory. In addition, measurements were started to determine the temperature dependent attenuation of the microstrip transmission line in the array as well as the effects of the multiple bias lead on the array. This work involved both the fabrication of samples specially designed to test these various properties as well as the development of computer software to simulate the predicted response of the circuits. The development of the computer interfacing and software needed for the conversion of our new SEM into an EBL system was now essentially complete, and we were now using this system, purchased with DOD URIP funds, for our mask fabrication.

During the sixth period the effects of a range of array parameters were studied in order to optimize the array design for higher power and to improve our understanding of its operation.

1. Parallel biased arrays with two independently biasable sections were fabricated and studied. The array could be operated with either one or both sections biased at the operating voltage. Measurements were made of load power as a function of which sections were in operation. It was observed that the load current with both sections operating was more than the sum of the currents of the two individual sections. This led to the

conclusion that the higher transmission line current when both sections were in operation produced additional phase alignment of the junctions. It was also observed that the two sections of the array phase-lock to each other. That is, the current through one section could be varied relative to the other over a certain range but the two sections would continue to operate at the same frequency. The strength of the phase-locking provided an independent measure of the amplitude of the load current, which was consistent with that measured by the detector junction. The overall power of these arrays continued to be in the $1 - 2\,\mu W$ range.

2. The shunted junctions in the array had both parasitic capacitance and inductance. Analytic results for the RSJ model thus did not exactly predict their performance. This was particularly important in our use of the amplitude of the Josephson current step to measure rf power. We carried out computer simulations based on more realistic junction models. We were confident, based on this refined analysis, that our power estimates were accurate within a factor of two.

3. It was discovered after considerable testing that there was a minimum base electrode thickness and a minimum critical current for which the arrays would operate. We did not have enough personnel to investigate this problem in more detail; however, it did explain why some of our earlier arrays did not work and enabled the fabrication of arrays which consistently operated with microwatt powers.

The work done on junction development (Pb alloy) during the seventh period was as follows:

1. Work was carried out to increase the critical current and I_cR products of our resistively shunted junctions. This was needed in order to obtain the higher power and operating frequencies which were required. To date it had been possible to increase I_c to 2.5mA and the I_cR product to 1.3mV in shunted junctions without heating or other problems degrading their performance.

2. The upper operating frequency for the lead alloy junctions was measured by

7

putting two junctions in a small loop in order to measure their phase locking as a function of frequency. Note that in the arrays the upper frequency limit is determined by the losses in the lead alloy transmission lines. This occurs at about half the cutoff frequency of the junctions. The frequency limit for our junctions, measured in a small loop, was 1 THz. This was the expected cutoff based on the measured gap voltage from the I-V curve. (The copper shunt under the junctions reduces the gap some from the standard value.)

3. Fabrication techniques were improved, permitting the fabrication of larger area junctions. The width of the junctions was successfully increased from 1μm to 4μm. The difficulty in doing this using our self-aligned masking technique was that the mask is suspended above the substrate for a span equal to the junction width. These greater width junctions, however, have several advantages. The greater area improves heat dissipation, permitting larger values of I_c. In addition, the reduced critical current density permits an increase in capacitance and thus in β_c, the damping parameter. This made it possible to achieve values of β_c needed for optimum locking strength among the junctions.

Our major result during period eight was the fabrication and testing of improved array designs making use of the developments in junction technology and in our understanding of array operation resulting from work earlier this year. Such an array gave a five fold peak power increase (to 7μW) over those tested earlier in the year. Power levels above 1μW were achieved for a number of frequencies in the range of 340 GHz to 440 GHz; however, the array was not continuously tunable throughout the range. A good understanding of the tuning range for these arrays needed to be developed. Work was progressing on the implementation of the Nb trilayer process for junction fabrication. We expected that the next major advance in array power would make use of these junctions since we were shifting emphasis from further improvements in lead alloy junctions to Nb — and probably then to NbN-junctions. At that time very high quality

8

Nb junctions with critical current densities up to about $1000A/cm^2$ were being fabricated. We were aiming to get this up to about $10^4A/cm^2$ but, more importantly, to develop techniques for making the junctions nonhysteretic at the frequencies of interest. This meant that we could not just import the process (or finished trilayers) from other labs but must develop processes tailored to our own needs.

The upper frequency limit of our arrays at that time was set not by the junctions but by the losses in the lead alloy microstrip. We worked with the group at JPL to make a "hybrid" array having an NbN ground plane and microstrip. In this work we did the design, mask fabrication anu junction fabrication, with JPL depositing and patterning the NbN film and dielectric layer. One complete sample was fabricated in this manner. This served mainly to highlight a number of refinements needed in the processing.

We have now succeeded in the fabrication and testing of a successful array using niobium junctions with aluminum oxide barriers. This array, which used the same design as our previous lead alloy arrays, generated a maximum power of about $1\ \mu W$ into a $20\ \Omega$ load. It operated over the same frequency range as the lead arrays and had an estimated linewidth of about 100KHz. The Nb junctions used had $700\ \mu A$ critical currents and were shunted with 0.5Ω low inductance ($\simeq 0.1$ pH) resistors. This critical current was still about a factor of 4 less than the maximum for our lead arrays, which accounted for the somewhat lower power.

Appendix A

1. Introduction.

There is a rapidly developing need for compact submillimeter sources for use in such applications as satellite communications and receivers for astronomical observation. Fundamental solid state oscillators such as Gunn or IMPATT diodes are presently limited to the millimeter wave range, leaving such bulky and power hungry sources as carcinotrons and CO_2 lasers which operate in some parts of the submillimeter range.

Josephson junctions are natural voltage controlled oscillators, and it has been recognized since the discovery of the Josephson effect that these junctions have the potential for filling this source gap at least up to frequencies of several terahertz. As the Josephson equations imply, the average frequency of supercurrent oscillation ν_0, which we call the Josephson frequency, in a junction is related to the dc component $\bar{V}$ of the voltage across the junction only through fundamental constants,

$$\bar{V} = \frac{h}{2e} \nu_0 \qquad (1.1)$$

where e is the charge on the electron and h is Planck's constant, so $2e/h = 483 \text{GHz/mV}$. Indeed this remarkable result has been shown (Tsai et al., 1983 and Jain et al., 1987) to be independent of the materials or structure of the junction to better than 1 part in 10^{16}. One would thus hope that Josephson junctions would be useful tunable sources operating up to the superconducting gap frequency — a few THz for conventional superconductors and perhaps tens of THz for the new high T_c materials.

Unless the junction voltage is constant in time, i e., $V(t) = \bar{V}$, Eq. 1.1 does not necessarily imply a pure sinusoidal oscillation with frequency proportional to the dc voltage. In practice, at high frequencies, it is usually easier to control the junction's bias current than its voltage. Indeed, there are many examples in the literature, such as chaotic behavior or periodic mode-locking to resonant structures, where, even though Eq. 1.1 is satisfied, almost none of the power generated by the junction is at the frequency ν_0.

Although a great deal of work in many laboratories has gone into the development of practical sources based on the Josephson effect, the serious problems related to the very low power and source impedance of individual junctions in addition to that of obtaining spectrally pure oscillation at the Josephson frequency have been difficult to surmount. One technique for overcoming these problems, which will be the focus of this chapter, is to use arrays of junctions in place of single junction sources. The discussion presented here has evolved from a lecture at the Nato Advanced Study Institute on Superconducting Electronics (Lukens, et al., 1989).

First, the properties of single junction sources will be reviewed in order to get a perspective on the problems to be solved. After a brief look at the performance expected from idealized arrays, perturbative techniques for analyzing arrays will be developed based on the resistively shunted junction (RSJ) model. While this model is clearly only approximately correct for real tunnel junctions, it can produce analytic results useful for achieving an insight into the design of coherent arrays. These results have proven to provide a very good description of many of the experiments to date. The final parts of this chapter will present a number of recent results for practical array sources where the junctions are distributed over many wavelengths as well as speculations on future directions for research.

2.   Single junction sources

2.1   Small junctions

The properties of single junction sources will be described first in order to see where arrays may be useful. The RSJ model (Fig. 1a) with C = 0 will be used to describe the junction's behavior since, for this case, analytic solutions exist which provide a useful insight. See e.g., Likharev, (1986) Chap. 4. When the bias current I_b is increased above I_c , the junction's phase ϕ begins to increase with time, producing an oscillating supercurrent (since $I_s = I_c \sin (\phi)$) and consequently an oscillating voltage. For I_b near I_c the voltage waveform is nearly a spike, having a large harmonic content. As I_c is

increased the higher harmonic content of the waveform decreases, giving a nearly sinusoidal wave for $\bar{V} \gtrsim V_c \equiv I_c R_J$. The amplitudes of the harmonics are given by

$$\tilde{V}_n \equiv V_c \tilde{v}_n = V_c \frac{2\bar{v}}{\left[(1+\bar{v}^2)^{\frac{1}{2}} + \bar{v} \right]^n} \tag{2.1.1}$$

where, $\bar{v} \equiv \bar{V}/V_c$ and $i \equiv I_b/I_c$ and for the RSJ model $\bar{V} = (i^2 - 1)^{\frac{1}{2}}$. Also, $\omega_c \equiv 2\pi V_c/\Phi_0$. This waveform approaches a nearly pure sinusoid for $\bar{v} > 1$. Since for most applications one would like a reasonably sinusoidal source, we will impose the constraint that $\bar{v} \gtrsim 1$ at the desired operating frequency.

Since the junction impedance at the Josephson frequency is $Z \simeq R_J$ for $\bar{v} \gtrsim 1$, at high frequencies the junction can be viewed as an oscillator of amplitude $\tilde{V}_1$ at the Josephson frequency in series with R_J as shown in Fig. 1b. The power available to a matched load from a single junction is then

$$P_1(\nu) = \frac{1}{8} \frac{\tilde{V}_1^2}{R_J} \rightarrow \frac{1}{8} I_c^2 R_J, \quad \bar{v} \gtrsim 1 \quad . \tag{2.1.2}$$

There are limits on both I_c and R_J which limit the maximum power obtainable at a given frequency. The discussion so far has assumed that the junction is one dimensional, that is, the phase difference between the electrodes is independent of the position on the electrode transverse to the direction of tunneling current flow. This, in general, means that the dimensions of the junction must be limited to assure a constant current density. Since the natural scale over which current density varies in the junction is the Josephson penetration depth $\lambda_J^2 = \hbar/(2e\mu_0 d J_c)$ (where d is the magnetic thickness of the barrier) keeping the junction's dimensions of order λ_J will assure the required uniformity. For an in-line junction with critical current density J_c, shown in Fig. 2, over a ground plane, the current is confined (on the x axis) within about $2\lambda_J$ of the end of the junction giving a maximum effective critical current in zero field of $I_c \simeq 2\lambda_J w J_c$ where w is the width of

12

the junction (Basovaish and Broom, 1975). As long as the current feeding the junction is uniform across the width of the junction (y axis), a solution exists in which the current density within the junction is also constant across its width for arbitrarily wide junctions.

At some point instabilities will develop in this uniform solution and limit the junction's width in practice. A very conservative estimate for this maximum stable width would be $2\lambda_J$. Then, since $\lambda_J^2 \propto 1/J_c$, the maximum critical current for a given material would be independent of J_c and equal to about 4mA for niobium. At the other extreme, very wide inline junctions are well known to have flux flow across the junction. One might expect this sort of instability to develop when the electromagnetic wavelength, λ_{em} , in the junction was equal to twice the junction width, that is at the first Fiske mode, since for this condition there will be where strong coupling between the Josephson and fluxon oscillations. Indeed it has been observed (Kautz, et al., 1987) that the phase-locking of junctions in voltage standard arrays to external radiation decreases abruptly for wider junctions. If the first instability is the first Fiske mode, then the maximum junction width will be given by

$$w_{em} = \frac{1}{2\nu \left(\mu_0 d C_s \right)^{\frac{1}{2}}}$$
(2.1.3)

where C_s is the specific capacitance. This width is independent of J_c but varies inversely with frequency. Thus the maximum critical current for this condition would depend on the critical current density but would decrease with frequency. For example, a niobium junction with a critical current density of $10^5 A/cm^2$ would have a maximum stable critical current of $I_c \simeq 7.6mA/\nu[THz]$.

Having fixed I_c , R_J should be adjusted using a shunt resistor depending on the desired operating frequency and limited, of course, by the material dependent intrinsic $I_c R_J$ product of the junction. The condition $\bar{v} \geq 1$ for a sinusoidal waveform limits the

maximum resistance for a given I_c and frequency ν. On the other hand, if R_J is reduced below the value for which $\bar{v} = 1$, Eq. 2.1.2 indicates that the power will decrease. Thus one should select the shunt resistance such that $R_J \approx \nu \, \Phi_0 / I_c$ giving

$$P_1(\nu) \approx \frac{1}{8} \, \nu \, \Phi_0 \, I_c \qquad (2.1.4)$$

Figure 3 illustrates the source resistance, critical current and available power as a function of frequency for single junction sources subject to the width constraints discussed above. For junctions with $w = 2\lambda_J$, one sees that the maximum single junction power is proportional to frequency with

$$P_1(\nu) \approx 1 \; (\nu[\text{THz}]) \; \mu\text{W} \qquad (2.1.5)$$

Thus, for example, one might expect a maximum power of about 1μW at 1THz. While this is sufficient for some applications, it is about the limit with proportionately less power available at lower frequencies. Also the source impedance for this 1μW source would be less than an ohm. This would require a substantial transformer ratio for typical loads and could be a problem if wide tuning were desired. Junctions with $w = \lambda_{\text{em}}/2$ have the potential for delivering above a microwatt at lower frequencies but at the expense of even lower source impedances.

2.2   Fluxon oscillators (wide junctions).

There are several groups which have reported significant power levels at frequencies up to several hundred gigahertz from fluxon propagation in very wide junctions. While the focus of this chapter will be on series arrays of junctions small enough to have a spacially uniform current density, we will briefly review these results for fluxon oscillators for the perspective which they provide on the possible advantages and disadvantages of this type of source.

Significant power has been observed from two different types of fluxon oscillators.

The first, which uses unidirectional flow, has been studied mainly in Japan (Yoshida, et al., 1989 and Nagatsuma, et al., 1983). In this type of oscillator, a magnetic field is applied in the plane of the junction, along the x axis (Fig. 2) to form flux vortices or fluxons in the junction. The bias current then forces the vortices to flow across the junction (along the y axis) along the transmission line formed by the base and counter electrodes. If the bias current is increased until the vortices are moving near the speed of light in the junction, voltage and thus the frequency becomes insensitive to small changes in the bias, i.e., the junction has very low differential resistance. The frequency can be tuned over a wide range by varying the vortex density in the junction by changing the applied field. It is estimated (Nagatsuma et al., 1983) that of the order of a microwatt of power should be available from such oscillators at frequencies ranging from about 100GHz to 1 THz and powers of this magnitude coupled to an SIS detector at the end of the junction transmission line have been reported up to 400GHz. A problem associated with this type of oscillator is that the characteristic impedance, which is that of the transmission line formed by the junction, is in general quite low. Transformers have been developed (Yoshida, et al., 1989) to couple power more efficiently to higher impedance loads and have succeeded in coupling about 0.1 μW to a 1 Ω load at 200GHz. The penalty for using these resonant transformers, however, is that the tuning range is severely restricted.

The second type of fluxon oscillator, which has been studied primarily by groups in Europe, has a similar geometry but uses a high Q resonant junction. These resonant fluxon oscillators are operated on their zero field steps, the operating frequency being determined by the dimensions of the junction rather than an applied field. Two groups have recently reported detecting power levels of the order of 0.1 μW from such junctions. One group (Cirillo et al., 1989) reported radiation at 75 GHz using on chip detection with small junctions. The oscillator junctions had a transmission line impedance of 1 Ω and an estimated available power of about 0.1 μW . Simulations show a steplike structure in junction's phase vs. time indicating a large harmonic content to the radiation as one might

15

expect from the picture of fluxons shuttling back and forth in the junction. A second group (Monaco et al., 1988 and Pagano et al., 1989) reported radiation near 10 GHz from an array of resonant fluxon oscillators in which a significant degree of phase-locking among the junctions was observed. In this case the radiation was coupled to a detector outside of the cryostat. Power levels of over 0.1 μW in a 50 Ω load were reported. In smaller arrays, where more complete locking could be achieved, linewidths of several kilohertz were observed.

2.3   Radiation linewidth

A final consideration related to single junction sources is their linewidth. The linewidth of the Josephson radiation is determined by frequency modulation due to low frequency voltage noise across the junction, (Likharev and Semenov, 1972) with frequencies up to about the linewidth $\Delta\nu$ being important. In terms of the current noise in the junction,

$$\Delta\nu = \frac{1}{2}\left(\frac{2\pi}{\Phi_0}\right)^2 S_I(0)\ R_d^2 \ . \qquad (2.3.1)$$

Here $S_I(0)$ is the low frequency current spectral density, and R_d is the differential resistance at the operating voltage. If $S_I(0)$ is just the Johnson noise current of the junction resistance R_J and $R_d \approx R_J$, then $\Delta\nu \approx 160$ MHz per ohm of junction resistance at 4 K . This is only a rough guide, since $S_I(0)$ will in general be increased due to such things as 1/f noise prevalent in high J_c junctions, as well as to down-converted quantum noise from near the Josephson frequency. On the positive side, since only low frequency noise is important in determining $\Delta\nu$, one can in principle make the linewidth arbitrarily small by shunting the junction at low frequencies without reducing its high frequency impedance. This technique has been successfully used (Smith et al., 1987), although it can have drawbacks such as the introduction of instabilities or chaotic behavior.

Another technique for linewidth reduction is to reduce the differential resistance of

the junction at the operating point through coupling to a resonant structure. An example of this is the fluxon oscillations in resonant wide junctions discussed above. These junctions can have very low differential resistance when biased on their zero field steps. The situation with unidirectional flux-flow is more complex. While the differential resistance is also small at the operating point, the junctions are tunable by varying the flux, so the linewidth will to some extent be affected by fluctuations of the flux linking the junctions, perhaps more than by spatially uniform fluctuations in the bias current.

One can summarize the properties of single junction sources by saying that, in general, such sources have either too little power, too low an impedance, too broad a linewidth or all of the above, although the power and impedance begin to become useful for some applications as terahertz frequencies are approached. Next we will take a brief, rather elementary look at small junction arrays to see to what extent the replacement of single junctions by arrays of junctions might solve these problems.

3.   Arrays

Interest in Josephson arrays was sparked in the late 1960's by experiments of Clark (1968) and a paper by Tilley (1970) who predicted superradiance in such arrays, much as in a collection of atoms in a cavity. One signature of this superradiance was a prediction that the output power would scale as the square of the number of junctions. This led to a hope — rather naive in retrospect — that significant power levels could be obtained from Josephson junctions simply by connecting a large number of junctions together without worrying in detail about just how they were coupled. The initial experiments were done by Clark (1973) and (1968) on two-dimensional arrays of superconducting balls, which were Josephson-coupled through their oxide coating as shown in Fig. 4b. Indeed, evidence of interactions among the junctions was seen; however experiments of this type have never produced significant levels of power. As will be seen later, when the details of how junctions phase-lock is discussed, for arrays of this type power is mostly dissipated in the array itself. The development of Josephson-effect arrays, involving hundreds of workers,

17

has been covered in detail in two review papers by Jain et al., (1984) (JLLS) and by Lindelof and Hansen (1984) and more recently in a book by Likharev, (1986). Readers are referred to these sources for a comprehensive review.

In more recent work, including successful attempts to obtain increased power from arrays of junctions, the junctions are simply treated as classical oscillators, i.e., the junction's current and phase are taken to be classical variables as in the discussion of single-junction sources above. This is the approach taken throughout this chapter. It is worth emphasizing the distinction between the present work based on the classical picture and the initial discussion of Josephson arrays in terms of superradiance, since much confusion has been caused over the years by not fully appreciating this distinction. This confusion has been compounded by the fact that there have been observations of the power from arrays increasing as N^2, as predicted for superradiance. As far as we know, all these observations can be explained in terms of purely classical circuit analysis, as will be seen, for example, below.

Probably the simplest example of the advantages to be gained from arrays of junctions can be seen by considering the one-dimensional array shown in Fig. 4a. Here a number of junctions are connected, e.g., by a transmission line, in series with each other and with the load to be driven, R_L, so that the rf current generated by a junction flows through all of the other junctions and the load. Representing each junction by its high frequency equivalent circuit (Fig. 1b), which to first order is not affected by the rf current, one sees that the array impedance can be matched to the load by taking the number of junctions to be $N = R_L/R_J$, thus solving the low impedance problem of single junction sources. For now it is simply assumed that all of the junctions will oscillate at the same frequency and in-phase. The discussion of the conditions needed for such phase-locking will occupy much of the remaining sections of this chapter. It will also be assumed for now that the circuit dimensions are small compared to the wavelength in the transmission line at the frequency of operation so that the lumped circuit approximation

18

can be used. The constraints on I_c and R_J discussed in Sec. 2 can then be used to estimate the number of junctions needed to match a 50 Ω load to an array designed to operate near a frequency ν, giving

$$N = \frac{R_L}{R_J} \approx \begin{cases} 100/\nu \, [\text{THz}], & w = 2\lambda_J \\ 200/\nu \, [\text{THz}]^2, & w = \lambda_{em}/2 \end{cases} . \qquad (3.1)$$

Here the two estimates for N correspond to the limits on the width of the small junctions as discussed in Sec. 2, taking $J_c = 10^5 \, \text{A/cm}^2$.

The available power from this one-dimensional array is just N times that available from a single junction in the array. Which, for the 50 Ω load is

$$P_N = N P_1 \approx \frac{1}{8} I_c^2 R_L \approx \begin{cases} 0.1 \, \text{mW} & w = 2\lambda_J \\ \dfrac{0.4 \, \text{mW}}{\nu [\text{THz}]^2} & w = \lambda_{em}/2 \end{cases} . \qquad (3.2)$$

If it is possible to match an array of any size to a load using a transformer, then the dependence of power on array size is linear in the number of junctions. The enormous impedance mismatch between a single junction and a typical load makes the use of transformers problematical, especially if much tuning range is to be preserved. Without transformers, situations occur where, when the number of junctions is varied, the load power varies as N^2. For example, this happens when the number of junctions is increased but the total array impedance is small compared to that of the load. An N^2 dependence also occurs if an array of junctions with $I_c < I_c$ max is matched to the load by reducing R_J as N increases such that $N R_J$ and $I_c R_J$ remain constant. Thus, for many practical situations the power from arrays is expected to increase as N^2. These situations are clearly purely classical in nature but are sometimes confused with superradiance.

Next, one could ask whether anything is gained by replacing the one-dimensional

19

array by a two-dimensional array, as in Figs. 4b-d. We imagine making such an array by replacing each junction in Fig. 4a by a parallel (transverse to the rf current) string of junctions, M junctions wide as in Fig. 4c. If all of these junctions were identical and all oscillated in phase, this would be equivalent to replacing each junction in Fig. 4a with a junction having $I'_c = MI_c$ and $R'_J = R_J/M$. One would then need M times as many of these series junctions to match the load; thus the power delivered to the load would be increased by a factor M^2.

As an example, at 1 THz approximately 100 junctions with $w = 2\lambda_J$ would be required in a one-dimensional array to match a 50 Ω load, producing in a power of 0.1 mW. If a two-dimensional array were used with a width M = 100, then the matched array would have 10^6 junctions and deliver 1 watt of power. It is not difficult to fabricate a million-junction array with modern lithographic techniques. The real question is whether all of the junctions could be made to oscillate in phase as assumed above, particularly since the motivation for thinking about a two-dimensional array is that the useful critical current of a single junction is limited due to phase instabilities that arise at larger values of I_c. Similar power estimates are obtained for the configuration shown in Fig. 4d.

The arrays discussed above (Figs. 4a, c, d) could all be called linear arrays, since for proper operation the phase should vary only in one direction, even in the two-dimensional arrays. It is important to distinguish this situation from truly two-dimensional arrays (Fig. 4b) where the phase varies in both dimensions. There has been a great deal of very interesting work, primarily to study phase transitions, in these latter arrays. This work will be completely ignored here, since it really does not address the problems related to using Josephson arrays as radiation sources.

4.   Phase-locking

It should be clear from the brief discussion above that the real key to the usefulness of arrays is how, or if, the junctions phase-lock. Even if all of the junctions are identical, one must still ask if the "uniform phase" condition (in which all junctions have the same

phase relative to the locking current) is a solution, and if so is it a stable solution. If there is such a stable solution, the next problem is to find out what happens if all of the junctions are not identical. In real arrays there is always some degree of scatter in the junction parameters, e.g., the critical current, as well as random noise, which tend to make the junctions of the array oscillate at different frequencies.

It is possible to get much insight into both the stability and strength of phase-locking in arrays by considering the well known phenomenon of a single junction phase-locking to external radiation. We will start by using perturbation theory to study the effects of external radiation on an RSJ for which analytic solutions are available. Later, the effects of junction's capacitance in the low β_c ($\beta_c \equiv \omega_c R_J C \leq 1$) limit will be included. The perturbation techniques used are standard and have been applied to Josephson junctions by several authors (Forder, 1977 and Kuzmin et al., 1981). Here the key ideas of the theory will be reviewed briefly and then applied to the phase-locking problem. To begin, a quantity related to the junction phase ϕ, called the "linearized phase", is defined by

$$\Theta = \hat{\omega} t \ , \tag{4.1}$$

where $\hat{\omega}$ is the junction's frequency averaged over a time long compared to a period of a Josephson oscillation, yet short enough to respond to the low frequency noise and modulation. The $\hat{\ }$ symbol is used in general to indicate averaging over the time scale which is long compared to $1/\omega$. The success of the perturbation theory depends on the wide separation of the Josephson frequency from the low frequency currents which are important in fixing the linewidth and oscillation frequency.

The essential results of the perturbation theory are shown schematically in Fig. 5 where the junction is represented by an equivalent circuit with two parts, one for the high frequency (HF) (near ω) behavior, and the second modeling the low frequency (LF) response. The high frequency circuit consists of the Josephson oscillator (with amplitude $\tilde{V}_1$ given by Eq. 2.1.1 and frequency ω) and the source impedance R_J. This HF section is

21

coupled to the LF section through ω, which is determined by the LF voltage through the Josephson equation (Eq. 1.1).

The perturbations which we wish to consider are caused by an rf current $\tilde{I}_T$ with a frequency near ω flowing through the HF terminals. This in turn affects the LF voltage (and thus ω) through the presence of a "mixing current,"

$$I_m = \alpha \left(2 \tilde{I}_T \cos \Theta \right) , \qquad (4.2)$$

in parallel with the bias and noise currents on the LF side. Here α is the conversion coefficient, which is given in the RSJ model as

$$\alpha = \frac{1}{2(1 + \bar{v}^2)^{\frac{1}{2}}} . \qquad (4.3)$$

The cause of this perturbation might, for example, be either an external rf current source or a load placed across the HF terminals, or both. So

$$\hat{\omega} = \hat{\omega}_u \left(\hat{I} + I_m \right) ,$$

(4.4)

where the subscript u refers to the value of the variable (ω) in the absence of the HF perturbation. In other words, in the presence of a HF perturbation the junction will oscillate at the same frequency as an unperturbed junction biased with a current equal to the sum of the bias and mixing currents in the perturbed junction.

In order to apply this technique to understand the phase-locking of a junction to external radiation, we take the perturbing rf current to be that due to an external current source with amplitude I_e and frequency ω_e near ω, so

$$\tilde{I}_T = I_e \cos \left(\omega_e t \right) . \qquad (4.5)$$

This gives a mixing current

$$I_m = \alpha \, I_e \cos (\delta\Theta) \; . \qquad\qquad (4.6)$$

where $\delta\Theta \equiv \Theta - \omega_e t$.

Equation 4.4 is actually a differential equation for Θ which can be rewritten by expanding $\omega(I)$ about I_b using the differential resistance of the unperturbed junction and remembering (Eq. 4.1) that $\dot\Theta = \hat\omega$. Thus,

$$\frac{\Phi_0}{2\pi R_d} \dot\Theta - \alpha \, I_e \cos (\delta\Theta) = \frac{\Phi_0}{2\pi R_d} \, \omega_u (\hat{I}) \; . \qquad\qquad (4.7)$$

If a new variable, $\theta \equiv \Theta - \omega_e t - \pi/2$ is defined, then Eq. 4.7 becomes

$$\frac{\Phi_0}{2\pi R_d} \, \dot\theta + I_L \sin \theta = \delta I \; , \qquad\qquad (4.8)$$

where I_L is

$$I_L = \alpha \, I_e \qquad\qquad (4.9)$$

and

$$\delta I = I_b - I_{be} \; . \qquad\qquad (4.10)$$

That is, δI is the difference between the actual bias current and the bias current I_{be} which would make the unperturbed junction oscillate at frequency ω_e. This equation is just the familiar equation for the phase of a RSJ with critical current I_L, resistance R_d and bias current δI; hence the solutions are well known.

The main result which we need is the locking strength, that is, the range of bias current over which $\dot\theta = 0$. Equation 4.8 clearly has a constant θ solution for $-I_L \leq \delta I \leq I_L$, with $0 \leq (\Theta - \omega_e t) \leq \pi$. Thus, as seen in Fig. 6a, $\bar{V}$ remains constant over a range of bias currents $2\,I_L$ about the bias current I_{be} for which the unperturbed junction would have frequency ω_e. Note that this locking strength could also be expressed in terms of the variation in I_c (since I_{be} is a function of I_c), which is possible at fixed bias without losing phase-lock. This latter view is more relevant for arrays where we may wish to bias a string of junctions with a common current and ask how large a scatter (e.g., in I_c) can be tolerated. In this sense a junction is most strongly locked when biased in the center of the

current step where the difference between the phase of the junction's oscillation and that of the external radiation is $\pi/2$, i.e., $\delta\Theta = \pi/2$. For this bias, the greatest deviation of I_c is possible in an arbitrary direction. The condition that the phase shift be $\pi/2$ for strongest locking has important implications for the design of arrays, as we shall see below. Another measure of locking strength is the variation in $\delta\Theta$ with δI. This is shown in Fig. 6b. Again one sees that $\delta\Theta$ is most stable with respect to changes in δI for $\delta\Theta = \pi/2$ and becomes completely unstable at the edges of the step, $\delta\Theta = 0$ or π. Note that for the range of negative $\delta\Theta$, where the current leads the oscillator phase, $d\delta\dot\Theta/d\delta\Theta > 0$; hence the phase-locked solution is unstable.

5.   Phase-locking in arrays

5.1   Locking strength within the RSJ model.

A detailed analysis of phase-locking in arrays has been carried out in JLLS (Chap.6), as well as in Likharev, (1986) (Chap. 13). The discussion presented here in terms of phase-locking to external radiation will, it is hoped, be intuitive while minimizing the mathematical complications. For large arrays this approach gives nearly the same results as does the more exact analysis. To begin, consider a series array of identical junctions, modeled by their HF equivalent circuits and connected in a loop through a load Z_ℓ as shown in Fig. 7. If all of the oscillators have the same phase, then the rf current which flows in series through all of the junctions and the load is

$$\tilde{I}_\ell = \frac{\tilde{V}_1}{R_J z_c} , \qquad (5.1.1)$$

where the coupling impedance per junction, z_c, is given in terms of the load impedance Z_ℓ and the junction impedance R_J as

$$z_c = \frac{1}{NR_J} (NR_J + Z_\ell) . \qquad (5.1.2)$$

To calculate how much the critical current of one of the junctions can be varied without having it come unlocked from the array, we can just treat this current as external radiation assuming that the array is large enough that a variation of the phase of a single junction

will have a negligible effect on $\tilde{I}_\ell$.

When all of the oscillators are running in phase, the relative phase of an oscillator and the locking current is fixed by the loop impedance. Since this impedance always contains a real part equal to the sum of the junctions' resistances plus the load resistance, it is clear that the ideal situation of having the locking current lag the oscillator phase by $\pi/2$ cannot be achieved for the circuit shown in Fig. 7 unless $\text{Im}(Z_\ell) \to \infty$. Thus, in optimizing $\text{Im}(Z_\ell)$ for the maximum locking strength, there is a tradeoff between the amplitude of the locking current and its phase, the phase being given by

$$p_\ell = \tan^{-1}\left[\frac{-\text{Im}(z_c)}{\text{Re}(z_c)}\right] . \qquad (5.1.3)$$

We now wish to see how far the bias current (or critical current) of the kth junction can be varied from the mean for the array without the junction coming unlocked. The mixing current for this junction, I_{mk}, is

$$I_{mk} = I_{k_L} \cos\left(p_\ell + \delta\Theta_k\right) , \qquad (5.1.4)$$

where $\delta\Theta_k \equiv \bar{\Theta} - \Theta_k$, $\bar{\Theta}$ being the mean phase of the oscillators, and

$$I_{k_L} = I_c \frac{\alpha \tilde{v}_1}{|z_c|} . \qquad (5.1.5)$$

Note that the product $\alpha \tilde{v}_1$ is a maximum near $\bar{v} = 1$, since $\tilde{v}_1 \propto \bar{v}$ for $\bar{v} \ll 1$ and $\alpha \propto 1/\bar{v}$ for $\bar{v} \gg 1$.

As for the case of a single junction locked to external radiation, phase-locking will be maintained for $-p_\ell \leq \delta\Theta_k \leq \pi - p_\ell$. Since $p_\ell \neq \pi/2$, it will be possible to shift I_{ck} farther in one direction than in the other. In a real array one would likely have a symmetric, roughly gaussian distribution of critical currents with the operating frequency of the array determined by the mean I_c of the distribution. In that case the maximum width which this

25

distribution could have and still maintain complete locking would be set by the lesser of the two deviations, i.e., by

$$\delta I_k \,[\text{max}] = I_L \min\{[1+\cos(p_\ell)], \, [1-\cos(p_\ell)]\} \ . \tag{5.1.6}$$

These phase relations are illustrated in Fig. 8.

Just as with a junction locking to external radiation, the stable situation is when the locking current lags the Josephson oscillator, i.e., the load must be inductive. The inductance which gives the largest locking strength can easily be determined by maximizing Eq. 5.1.6 with respect to L. If the load impedance is $Z_\ell = R_\ell + jL\omega$, then the locking strength is a maximum for

$$L\omega = \sqrt{3}\,(NR_J + R_\ell) \ , \tag{5.1.7}$$

so for strong locking the coupling impedance must have a large reactive component with an inductive character. One can also see the importance of this reactance by calculating the variation in $\delta\Theta_k$ with changes in I_{bk} from Eq. 5.1.4. Near equilibrium($\delta\Theta_k = 0$) this variation is

$$\left[\frac{\partial\delta\Theta_k}{\partial I_k}\right]^{-1} \propto |\tilde{I}_\ell|\sin(p_\ell) \propto \frac{\sin(p_\ell)}{|z_c|} \ , \tag{5.1.8}$$

i.e., the phase stability is proportional to the Im(y_c), where $y_c = 1/z_c$. Subject to this constraint the maximum power will be delivered to R_ℓ when $R_\ell = NR_J$. Thus $L\omega = 2\sqrt{3}\,NR_J$ gives $p_\ell = \pi/3$ and a value for δI_k [max] of

$$\delta I_k \,[\text{max}]\,/I_c = \frac{\alpha\,\tilde{v}_1}{8} \ . \tag{5.1.9}$$

Using the RSJ values for α and $\tilde{v}_1$ with $\bar{v} = 1$ gives

$$\delta I_k \,[\text{max}]\,/\,I_c \simeq .04 \ . \tag{5.1.10}$$

26

Therefore, the total spread in I_{bk} for this type of array can be about 8% before junctions will start to unlock. Since I_b / I_c is about 1.4 (in the RSJ model) for $\bar{v} = 1$, this implies a permissible variation in I_c of about 10%. This number is a maximum since the spread of I_c for the junctions near the center of the distribution will produce some scatter in their phases with a consequent small reduction in the locking current $\tilde{I}_\ell$.

If we are concerned about the unlocking of the first few junctions in the tails of a large distribution, the estimate above is rather close, as can be shown from computer simulations (Sauvageau, 1987). It is worth noting that the interaction range of the junctions in this type of array is essentially infinite, i.e., the interaction of the kth and ℓ^{th} junctions does not depend on their separation. As a consequence, the unlocking of several junctions in a large array has a negligible effect on the phase locking among the remaining junctions. It may be undesirable to have even one junction unlocked, however, since if its frequency is close enough to that of the array, mixing will occur which will modulate the array frequency to some degree. As the width σ of the I_c distribution is increased and additional junctions unlock, $\tilde{I}_\ell$ will begin to decrease, causing yet more junctions to unlock and leading to a rapid uncoupling of the array with increasing σ. Computer simulations on a 40-junction array show that this "catastrophic" failure occurs for a value of σ about twice that at which the junctions in the tail of the distribution first unlock.

We conclude this section with some brief comments on the prospects for 2D linear arrays. As discussed above, when RSJ's are connected in an inductive loop, their rf voltage tends to add in-phase around the loop. For the 2D arrays shown in Figs. 4b, c, the lowest impedance path seen by a junction is the inductive path through the junction in parallel with it. For these configurations the tendency is for the rf polarities to change along a parallel chain of junctions with the result that circulating currents are set up within the chain. Hence power is dissipated internally instead of being coupled to the load. For the 2D array in Fig. 4d, on the other hand, the lowest impedance path for all of the series chains is the (presumably inductive) path through the load. Consequently, one

27

would expect a constant phase transverse to the current flow, as desired, for this array. Capacitive coupling between the chains might further stabilize this situation. These stability arguments are developed in much greater detail in JLLS.

5.2   Radiation linewidth of arrays.

Each junction of an array has an intrinsic noise current $S_{I_k}(0)$ which tends to vary the junction's voltage and thus the array's frequency. In the discussions above, we determined the phase-locking effect of the array on a single junction of the array by treating the remaining N-1 junctions as a fixed frequency external source. In this approximation the frequency of the perturbed junction clearly would not change as long as it remained phase-locked to the array. Thus no information is provided about the linewidth. The more exact treatment needed to calculate the linewidth is given in JLLS Chap. 6. Again, one starts from Eq. 4.4. However, the mixing current for the kth junction, $(I_m)_k$, is now calculated using the rf current obtained by explicitly summing the rf voltage due to all of the other junctions, whose frequencies can now depend on the bias current of the kth junction. Considering an array of N identical junctions as in Fig. 9, this analysis yields an almost intuitive result: Changing the effective low frequency bias current $(I_e)_k \equiv (I_B)_k + (I_n)_k + (I_m)_k$ of the kth junction while keeping that of the other N-1 junctions fixed, i.e., $R_s \gg NR_J$, changes the low frequency voltage of the kth junction (and thus the rest of the arrays since all junctions are phase-locked) by a factor $1/N$ of that obtained if the junction were not coupled to the array. That is,

$$\delta V_A = \frac{1}{N} (R_d)_k \, \delta(I_e)_k . \qquad (5.2.1)$$

From Eq. 2.3.1, $\Delta \nu \propto R_d^2$, so this reduction of the differential resistance due to phase-locking would narrow the linewidth by a factor N^2 . However, there are N noise sources, so their incoherent sum results in an effective noise current with low frequency spectral density $S_I(0) \propto N$, giving for the linewidth, $\Delta \nu_A$, of the phase-locked array,

$$\Delta\nu_{\text{A}} = \frac{1}{N}\, \Delta\nu_{\text{J}} \tag{5.2.2}$$

where $\Delta\nu_{\text{J}}$ is the linewidth of a junction when it is not coupled to the array. For example, while a single $0.1\ \Omega$ junction would ideally have a linewidth of about $16\ \text{MHz}$, an array of say 1000 such junctions should have a $16\ \text{KHz}$ linewidth. If the junctions' resistance is varied along with N so that the total array impedance NR_{J} remains constant, the linewidth would vary as $1/N^2$, e.g., a single $100\ \Omega$ junction should have a linewidth of $16\ \text{GHz}$! As we shall see next, even greater reductions in linewidth are possible if the effects of low frequency shunting are taken into account.

Consider the case where the low frequency shunt $R_s \ll NR_d$. Then one can see from Fig. 9 that the noise voltage generated by the junctions' noise currents is largely shorted by R_s giving an intrinsic linewidth $\Delta\nu_{\text{A}_i}$ of

$$\Delta\nu_{\text{A}_i} \simeq \frac{1}{N^3}\, \Delta\nu_{\text{J}} \left(\frac{R_s}{R_d} \right)^2. \tag{5.2.3}$$

If one takes $R_s \simeq R_d$ this implies a dramatic linewidth reduction in large arrays — by a factor of N^3! This soon reaches the point where the intrinsic noise will be dominated by coherent noise sources, e.g., by the Johnson noise voltage generated by R_s. Since this voltage is divided equally across all the junctions in a phase-locked array, $S_v(0) \propto 1/N^2$, giving a factor N^2 reduction in linewidth $\Delta\nu_{\text{A}_s}$ due to the shunt. So,

$$\Delta\nu_{\text{A}_s} \simeq \frac{1}{N^2}\, \Delta\nu_s \,,\ \ \Delta\nu_s \equiv \frac{1}{\pi} \left(\frac{2\pi}{\Phi_0} \right)^2 k_{\text{B}} R_s T_s \tag{5.2.4}$$

where T_s is the temperature of the shunt and $\Delta\nu_s$ is the linewidth a single junction would have if its voltage noise were that produced by R_s. This is worth noting since it implies that, in large arrays, there may not be a penalty in linewidth for using noisy, e.g.,

high J_c , junctions.

A possibly severe penalty for the use of low impedance shunts is the large increase in bias and cooling power which they can require. Since, roughly speaking, only noise up to frequencies $\Delta\nu$ contributes to $\Delta\nu$, a shunt in a large array must only be effective at very low frequencies. A rather large inductance should thus be tolerable in series with the shunt resistor, making it possible to place this resistor, for example, at 77 K . While this would increase the linewidth due to the shunt, this linewidth would still be so small as to be acceptable for most applications.

Experimental evidence for the predicted dependence of power and linewith on array size is shown in Fig. 10 taken from the result of JLLS. Here arrays of 0.1 Ω microbridge junctions incorporated in a 50 Ω microstrip were measured. The power is seen to increase as N^2 as is expected for the coherent state of this array, since the array impedance is always much less than that of the load (see Sec. 2). Since the low frequency shunting in this array is negligible, the linewidth is expected to vary as 1/N as observed.

5.3   Effects of capacitance on phase-locking in arrays.

So far only junctions with no capacitance have been considered. In this section we will examine what changes in the behavior of arrays one might expect if $\beta_c{\neq}0$. One must to be aware that capacitance is dangerous. A clue to this is seen in the locking of a single junction to external radiation where the situation corresponding to a capacitive load, i.e., the current phase leading the oscillator, is unstable. It has been shown that for an array like that in Fig. 7, the uniform phase solution is unstable if Z_ℓ is capacitive (Jain et al., 1984 and Likharev, 1986). Instead, the rf voltage tends to sum to zero around the loop. Further, there are many examples of chaotic behavior in capacitive junctions subject to applied radiation or external loads. In spite of this there are several reasons to consider using capacitive junctions in arrays.

Potential advantages of capacitive junctions are: By far the most advanced technology for making Josephson junctions is for tunnel junctions where capacitance is

unavoidable. Also, as we shall see below, the presence of a small shunt capacitance can, under certain conditions, enhance the locking strength in the array. Indeed, there have been very successful examples of locking large arrays of high capacitance tunnel junctions to external radiation, (Kautz et al., 1987) as well as demonstrations that even junctions with $\beta_c \gg 1$ can phase lock and generate radiation (Finnegan and Wahlsten, 1972, Lee and Schwarz, 1984, Lee and Schwarz, 1986, Kuzmin et al., 1987, Krech and Reidel, 1987, and Smith et al., 1987). Furthermore, it has been shown that tunnel junctions generate significant power levels, at least up to the sum of the gap frequencies (Robertazzi et al., 1988). Fortunately, a very general technique for analyzing the stability of the uniform solution in arrays with arbitrary β_c and Z_ℓ has been developed by Hadley, Beasley and Wiesenfeld (HBW) (Hadley et al., 1988 a, b). This should be of great help in desig ning arrays of capacitive junctions to avoid the "dangerous" regions of parameter space.

In this section the analysis above for arrays of junctions with C = 0 will be extended, using perturbation theory, to the case of small C, i.e., for $\beta_c \lesssim 1$, in order to develop some insight into the effects of capacitance. This low C region near $\bar{v} \gtrsim 1$, where one can still hope to obtain meaningful results from perturbation theory, is also the region in which the analysis of HBW indicates that the uniform solution should have the greatest stability.

In order to include the effects of junction capacitance, a capacitor will be connected across the HF terminals of the junction and treated as an additional perturbation. The details of this analysis, which is summarized below, are shown in more detail in Lukens, et al., (1989). The effects of the various perturbations to the junction are additive, since the circuits are linear. The direct effect of the shunt capacitor on the junction will be to change the voltage $\bar{V}$ obtained for a given bias current. This will be ignored since to first order it does not influence the locking behavior of the junction, but just means that a slightly different bias must be used to achieve the desired frequency. The most important effects of the capacitance are to change the effective impedance and rf voltage of the

31

junction as seen by the rest of the circuit. This is illustrated in Fig. 11.

These junctions are now connected in a loop in series with a resistive load having a resistance, in units of NR_J, or r_ℓ. The phase shift between the junctions' oscillators and the loop current $\tilde{I}_\ell$ produced by the shunt capacitance is $p_\ell = \tan^{-1}[-\beta_c\bar{v}r_\ell/(r_\ell + 1)]$, which has the same sign as that due to an inductance in series with the load. Thus the phase relationship between the loop current and the oscillators is that required for stable locking, even with a purely resistive load. The fraction of $\tilde{I}_\ell$ which flows through R_J, $\tilde{I}_{\ell R}$, is responsible for the phase-locking. $\tilde{I}_{\ell R}$ is further shifted with respect to $\tilde{I}_\ell$ by a phase $\tan^{-1}(-\beta_c\bar{v})$ giving a total phase shift $p_{\ell R}$ between the oscillators and $\tilde{I}_{\ell R}$ which can exceed $\pi/2$. These phase relations are illustrated in Fig. 12 and show a potential advantage of the shunt capacitance over a series inductance. Recall from section 5.1 that the locking strength and hence the acceptable scatter in I_C was substantially reduced, since it was not possible to have a $\pi/2$ phase shift between the mean phase of oscillators and the locking current. With a shunt capacitance one can achieve this optimum phase shift by choosing $\beta_c\bar{v} = \left[\dfrac{1 + r_\ell}{r_\ell}\right]^{\frac{1}{2}}$.

There is a large parameter space in $\bar{v}$, β_c and Z_ℓ that can be explored to optimize the power and locking strength for a given application. To get a feel for the performance of these arrays with $\beta_c > 0$, let us take the purely resistive load which maximizes the load power for given β_c and $\bar{v}$. This gives

$$r_\ell = \left[1 + (\beta_c\bar{v})^2\right]^{-\frac{1}{2}} . \tag{5.3.1}$$

The desired $\pi/2$ phase shift is then obtained for $\beta_c\bar{v} = \sqrt{3}$. For these values the locking strength is

$$\delta I_k / I_c = \frac{\alpha\tilde{v}_1}{2\sqrt{3}} . \tag{5.3.2}$$

32

This is more than twice that for the RSJ array from Eq. 5.1.9, indicating that complete locking should still be possible with a total spread in I_c of greater than 20%. For smaller values of $\bar{v}$ the limits of perturbation theory are being pushed, so the exact values need to be compared with computer simulations. We note that the estimate from perturbation theory is in line with the result of simulations done by HBW on 100-junction arrays with $\beta_c \simeq 0.75$ and $i \simeq 2.3$, where locking was still observed with a scatter greater than 15% in R_j, C and I_c.

6.   Distributed arrays

In all of the discussions above, it has been assumed that the dimensions of the arrays were much less than the wavelength λ. As a result, the lumped circuit approximation could be used. To see if this is realistic, note that if the entire array is to have a length less than $\lambda/8$ the junction spacings must be

$$ s = \frac{1}{8}\frac{v_p}{\nu N} \simeq 0.1 \ \mu m \ , $$

(6.1)

where $v_p \simeq 10^8 \, m/s$ is the propagation velocity in the superconducting transmission line connecting the junctions, and the value of νN from Eq. 3.1 has been used. Unfortunately, 0.1 micron spacing is about two orders of magnitude closer than is practical to place the junctions in the array when such things as heating and the limits of lithography are considered. We conclude that in order to achieve maximum power, even from one-dimensional arrays, the junctions must be distributed over a wavelength or more.

The analysis of phase-locking above has shown that the phase of the junction's oscillations relative to the locking current flowing in the coupling circuit is crucial. In general, an oscillator in a transmission line will generate waves propagating in both directions. This makes it impossible to maintain the same phase relationship between all of the oscillators and the locking current when the junctions are placed at arbitrary

positions along the transmission line. There have been several proposals (Jain et al., 1984, Davidson, 1981, and Sauvageau et al., 1987 a) for placing junctions along a transmission line such that they will phase-lock. The simplest approach, described in this section, is just to place the junctions at wavelength intervals along the transmission line. Hence, all junctions see the same impedance and the same relative phase. The analysis of this circuit at the frequency ν_λ, where the spacing is equal to λ, is identical to the lumped circuit analysis above. The disadvantage of this approach is that it is only valid at a discrete set of frequencies. It is therefore not clear that such an array will be continuously tunable over a large range of frequencies.

Figure 13 shows a schematic of such a distributed array. The junctions (indicated by ×) are placed at λ intervals along a serpentine microstrip transmission line. An independently biased detector junction is placed immediately after a load resistor in the line. By measuring the range of detector bias current over which the detector phase locks to the array-generated locking current flowing through the load resistor, the power to the load can be determined for each operating frequency of the array. The ends of the array are terminated with $\lambda/4$ stubs so that, to the junctions, the array appears grounded through the load resistor. Additional length can be added to the stub in order to add a reactive component to the load to optimize the locking strength.

The current amplitude of the Josephson step in the detector junction of such an array is shown in Fig. 14 as a function of the average frequency of the array junctions as determined by measuring the dc voltage across the array (Sauvageau et al., 1987 b). This array contained 40 junctions, which were biased in series, with the bias current flowing through the microstrip. The junctions were separated by 1 mm of microstrip giving an expected value for ν_λ of 100 GHz. Indeed a sharp peak in rf current $\tilde{I}_\ell$ through the detector is observed at 108 GHz indicating the presence of phase-locking near this frequency. The peak value of the rf current, however, is that expected if only seven of the forty junctions were locked in-phase. It is possible to directly measure the distribution of

34

critical currents of the junctions in the array; the resulting distribution is in fact too broad for complete locking. From the measured maximum rf current and the distribution of I_c's, one concludes that only seven or eight of the junctions could be phase-locked. Thus the data show that the junctions which are sufficiently uniform to lock, lock with very nearly the same phase, as predicted.

Since our fabrication process does not yield sufficiently uniform critical currents to insure that locking would be achieved if all junctions were biased with the same current, a "parallel" bias scheme has been used. The superconducting bias leads inject (remove) current at alternate bends in the microstrip, as seen in Fig. 15, with the result that each junction is part of two interlocking dc SQUIDs. All junctions then have the same average voltage, which alternates in polarity along the microstrip. This forces the bias current to divide so as to compensate to first order for the variations in the junctions' critical currents. The rf locking current is still crucial however, since without it the phase of each junction would be essentially random due to random flux linking the SQUIDs. Further, noise currents would cause voltage (and frequency) fluctuations among the junctions. Phase-locking for this type of parallel biasing has been analyzed in detail in JLLS. It is primarily as discussed above for series-biased junctions except that the effective scatter in I_c approximately equals Φ_0/L, where L is the inductance of the dc SQUID. For this circuit $\delta I_c \simeq 5\ \mu A$. The junctions are resistively shunted lead-alloy tunnel junctions having an area of about $1.5\ \mu m^2$. These resistively shunted junctions, which have $I_c = 2.5 mA$, have been described in detail elsewhere (Sauvageau et al., 1987 a).

The junctions' separation in this array is $350\ \mu m$ giving a value for ν_λ of 350 GHz. The power (as determined from the rf current through the detector and the 23 Ω load resistor) vs. frequency is shown in Fig. 16. Significant power is observed starting at about ν_λ, however the array also generates over $1\ \mu W$ of power at a number of discrete frequencies over a band from 340 GHz to 440 GHz , where the junctions are not separated by integer wavelengths. The maximum power of $7\ \mu W$ is consistent with all 40

junctions of the array locked in-phase. Other arrays with lower critical current junctions are continuously tunable through this band delivering more than 1 μW of power (Wan, et al., 1989 a,b), again consistent with all junctions in-phase.

7. Prospects for the future.

As of this writing, the distributed arrays described above are the most powerful fundamental solid state sources at 400 GHz. Rather straightforward, though technically complex, extensions of that work should result in sources operating at over 1 THz with nearly 1 mW of power. Clearly, much work — both experimental and theoretical — needs to be done. This is especially true when considering wide $(w \simeq \lambda_{em}/2)$ junctions and two-dimensional arrays, where there are essentially no experimental results at present. Probably the most immediate problem is to couple the submillimeter radiation off chip to determine its spectral purity. Fortunately, very broadband antennas have recently been demonstrated in this frequency range (Büttgenbach et al., 1988 and Li et al., 1988) for use with superconducting SIS mixers. Also, more theoretical work is needed to understand the unexpectedly wide tuning range seen in many of the distributed arrays.

Table I summarizes the range of powers and linewidths which might be expected from several different types of arrays, based on the discussions in this chapter. These range from one-dimensional, unshunted arrays of narrow junctions in the upper left of the table, to two-dimensional, linear arrays of the type shown in Fig. 4c, with low frequency shunts, at the lower right. Essentially the projections in the upper left are rather straightforward extrapolations of present design, while, moving to the lower right, one ventures into a territory with progressively more ideas which have yet to be tested. It would, for example, be surprising if a 1 Hz linewidth at one terahertz were ever achieved.

Finally, it is worth considering what impact the new copper oxide superconductors (HTS) might have on the development of these array sources. The most straightforward application of these materials could be as superconducting ground planes and transmission lines. For a given type of conventional superconductor, e.g., niobium, transmission lines

become very lossy at half of the upper frequency limit for the junctions' oscillation. Thus the upper frequency limit might be doubled using HTS microstrip, e.g., to about 3 THz using NbN junctions. While making high quality tunnel junctions of HTS material may be some time in the future, it is worth remembering that the array oscillators do not require good tunneling characteristics. Junctions, e.g., microbridges, with a normal metal barrier should work well; preliminary reports of such thin film junctions which show the Josephson effect have already been presented (Schwartz et al., 1989). While the use of HTS junctions may well extend the upper frequency limit of Josephson effect sources to above 10 THz, the most important advantage initially should be to permit operation at 77 K and thus enhance compatibility with many semiconductor systems. From all of this, we see that Josephson sources have a great, perhaps unique, potential for filling a real void throughout the submillimeter wave band.

8.   Acknowledgements.

References

Basovaish, S. and Broom, R.F. (1975). Characteristics of in-line Josephson tunneling gates. IEEE Trans. Magn., MAG-11, 759-762.

Büttenbach, T.H., Miller, R.E., Wengler, M.J., Watson, D.M., and Phillips, T.G. (1988). A broad-band low-noise SIS receiver for submillimeter astronomy. IEEE Trans. Microwave Theory Tech. 36, 1720-1726.

Cirillo, M., Modena, I., Carelli, P., and Foglietti, V. (1989). Millimeter wave generation by fluxon oscillations in a Josephson junction. J. Appl. Phys., in press.

Clark, T.D. (1968). Experiments on coupled Josephson junctions. Phys. Lett. A 27, 585-586.

Clark, T.D. (1973). Electromagnetic properties of point-contact Josephson junction arrays. Phys. Rev. B 8, 137-162.

Davidson, A. (1981). New wave phenomena in series Josephson junctions. IEEE Trans. Magn., MAG-17, 103-106.

Finnegan, T.F. and Wahlsten, S. (1972). Observation of coherent microwave radiation emitted by coupled Josephson junctions. Appl. Phys. Lett. 21, 541-544.

Forder, P.W. (1977). A useful simplification of the resistively shunted junction model of a Josephson weak-link. J. Phys. D 10, 1413-1436.

Hadley, P., Beasley, M.R., and Wiesenfeld, K. (1988 a). Phase-locking of Josephson junction arays. Appl. Phys. Lett. 52, 1619-1621.

Hadley, P., Beasley, M.R., and Wiesenfeld, K. (1988 b). Phase-locking of Josephson junction series arrays. Phys. Rev. B 38, 8712-8719.

Jain, A.K., Likharev, K.K., Lukens, J.E., and Sauvageau, J.E. (1984). Mutual phase-locking in Josephson junction arrays. Phys. Rep. 109, 309-426.

Jain, A.K., Lukens, J.E., and Tsai, J.-S. (1987). Test for relativistic gravitational effects on charged particles. Phys. Rev. Lett. 58, 1165-1168.

Kautz, R.L., Hamilton, C.A., and Lloyd, Frances L. (1987). Series-array Josephson voltage standards. IEEE Trans. Magn., MAG-23, 883-890.

Krech, V.W. and M. Reidel (1987). Synchronisationseffekte in Anordnungen aus zwei Josephson Verbindungen mit endlichem McCumber-Parameter. Ann. Phys. (Leipzig) 44, 329-339.

Kuzmin, L.S., Likharev, K.K., and Ovsyannikov, G.A. (1981). Mutual synchronization of Josephson contacts. Radio Eng. & Electron. Phys. 26, No.5, 102-110.

Kuzmin, L.S., Likharev, K.K., and Soldatov, E.S. (1987). Experimental study of mutual phase locking in Josephson tunnel junctions. IEEE Trans Magn., MAG-23, 1051-1053.

Lee, G.S. and Schwarz, S.E. (1984). Numerical and analytical studies of mutual locking of Josephson tunnel junctions. J. Appl. Phys. 55, 1035-1043.

Lee, G.S. and Schwarz, S.E. (1986). Mutual phase locking in series arrays of Josephson tunnel junctions at millimeter-wave frequencies. J. Appl. Phys. 60, 465-468.

Li, X., Richards, P.L., and Lloyd, F.L. (1988). SIS quasiparticle mixers with bow tie antennas. Int. J. Infrared & Millimeter Waves 9, 101-133.

Likharev, K.K. and Semenov, V.K. (1972). Fluctuation spectrum in superconducting point junctions. JETF Lett. 15, 442-445, reprinted from 2hETF Pis. Red. 15, No. 10, 625-629.

Likharev, K.K. (1986). Dynamics of Josephson Junctions and Circuits. Gordon and Breach, New York, Chap. 13.

Lindelof, P.E. and Hansen, J. Bindslev (1984). Static and dynamic interactions between Josephson junctions. Rev. Mod. Phys. 56, 431-459

Lukens, J.E., Jain, A.K., and Wan, K.-L. (1989). Application of Josephson effect arrays for submillimeter sources. Proceedings of the NATO Advanced Study Institute on

Superconducting Electronics (Nisenoff, M. and Weinstock, H., eds.). Springer-Verlag, Heidelberg. To be published.

Monaco, R., Pagano, S., and Costabile, G. (1988). Superradiant emission from an array of long Josephson junctions. *Phys. Lett. A* 131, 122-124.

Nagatsuma, T., Enpuku, K., Irie, F., and Yoshida, K. (1983). Flux-flow-type Josephson oscillator for millimeter and submillimeter wave region. *J. Appl. Phys.* 54, 3302-3309.

Pagano, S., Monaco, R., and Costabile, G. (1989). Microwave oscillator using arrays of long Josephson junctions. *IEEE Trans. Magn.*, MAG-25, 1080-1083.

Robertazzi, R.P. and Buhrman, R.A. (1988). NbN Josephson tunnel junctions for terahertz local oscillators. *Appl. Phys. Lett.* 24, 2441-2443.

Sauvageau, J.E., Jain, A.K., Lukens, J.E., and Ono, R.H. (1987 a). Phase-locking in distributed arrays of Josephson oscillators. *IEEE Trans. Magn.*, MAG-23, 1048-1050.

Sauvageau, J.E., Jain, A.K., and Lukens, J.E. (1987 b). Millimeter wave phase-locking in distributed Josephson arrays. *Int. J. of Infrared & Millimeter Waves* 8, 1281-1286.

Sauvageau, J.E. (1987). Phase-locking in distributed arrays of Josephson junctions. Ph.D. dissertation, State University of New York at Stony Brook. Unpublished.

Schwartz, D.B., Mankiewich, P.M., Howard, R.E., Jackel, L.D., Straughn, B.L., Burkhardt, E.G., and Dayem, A.H. (1988). The observation of the ac Josephson effect in a $YBa_2Cu_3O/Au/YBa_2Cu_3O_7$ junction. *IEEE Trans. Magn.*, MAG-25 1298-1300.

Smith, A.D., Sandell, R.D., Silver, A. H., and Burch, J.F. (1987). Chaos and bifurcation in Josephson voltage-controlled oscillators. *IEEE Trans. Magn.*, MAG-23, 1267-1270.

Tilley, D.R. (1970). Superradiance in arrays of superconducting weak links. *Phys. Lett. A* 33, 205-206.

Tsai, J.S., Jain, A.K., and Lukens, J.E., (1983). High-precision test of the universality of the Josephson voltage-frequency relation. *Phys. Rev. Lett* 51, 316-319.

Wan, K.-L., Jain, A.K., and Lukens, J.E. (1989 a). Submillimeter wave generation using Josephson junction arrays. *IEEE Trans. Magn.*, MAG-25, 1076-1079.

Wan, K.-L., Jain, A.K., and Lukens, J.E. (1989 b). Submillimeter wave generation using Josephson junction arrays. *Appl. Phys. Lett.*. To be published.

Yoshida, K., Qin, J., Enpuku, K. (1989). Inductive coupling of a flux-flow type Josephson oscillator to a stripline. *IEEE Trans. Magn.*, MAG-25, 1084-1087.

Table 1

Prospective Sources at 1 Terahertz[2]

Array dimension	1	1	2
Junction (array) width	$2\,\lambda_J\ (2\lambda_J)$	$\lambda_{em}/2\ (\lambda_{em}/2)$	$\lambda_{em}/2\ (\lambda_t/2)$
$J_c\ [A/cm^2]$	X	2×10^6	2×10^6
$I_c\ [mA]$	4	40	40
Number of junctions	100	1000	10^6
Power [mW]	0.1	10	10^4
Linewidth (no LF shunt)	5 MHz	50 KHz	50 Hz
Linewidth (1 Ω LF shunt)	20 KHz	200 Hz	< 1 Hz

a) Estimates are based on parameters for nonhysteretic NbAlNb junctions with effective length $2\,\lambda_J$. A 50 Ω load is assumed. λ_t is the wavelength in the transmission line.

Figure Captions

Fig. 1.   a) Equivalent circuit model for resistively shunted junctions (RSJ) with bias current I_b, noise current I_N, shunt resistance R_J and capacitance C and supercurrent $I_s = I_c \sin\phi$. b) Equivalent circuit for frequencies near ν_0.

Fig. 2.   Diagram of in-line junction. a) Edge view showing $J_c(x)$ concentrated within $2\lambda_J$ of end of junction. b) Top view. Tunnel barrier is enclosed by dashed lines. Regions of non-zero tunneling current are shown by ⊙.

Fig. 3.   Properties of single junction sources design for maximum available power at a given frequency subject to the width constants $w = 2\lambda_J$ (--- narrow) and $w = 0.5\,\lambda_{em}$ (—— wide), and for both cases $J_c = 10^5 A/cm^2$ and length is $2\lambda_J = 2\mu m$. For narrow junctions the frequency independent values of I_c and w are indicated on the axes (- - -). The available power of the wide junction is also frequency independent as shown on the power axis.

Fig. 4.   a) High frequency equivalent circuit for a one-dimensional array. b-d) Possible junction connections for two-dimensional arrays.

Fig. 5.   Equivalent circuit for the RSJ model from perturbation theory. Low frequency (LF) section models response for $\omega \ll \omega_J$ ($\omega_J = 2\pi\dot{V}/\Phi_0$) and is coupled to the high frequency (HF) section by the mixing current I_m — see text. HF section contains the Josephson oscillator $\tilde{V}_1 \cos\omega_J t$ and source impedance R_J. The perturbation consists of an rf current $\tilde{I}_T$ with $\omega \sim \omega_J$ flowing through the HF terminals.

Fig. 6.   a) Junction I-V curve in neighborhood of radiation induced step. b) Phase-locking stability along step, $[\partial\delta\Theta/\partial\delta I]^{-1}$. Note greatest stability is for $\delta\Theta = \pi/2$. The region $0 > \delta\Theta > -\pi$ is unstable.

Fig. 7.   Equivalent HF circuit for an array terminated in load Z_ℓ.

Fig. 8.   Relative phase of the mean oscillator voltage (real axis), load current $\tilde{I}_\ell$ and k^{th} junction with different bias or critical current for array modeled in Fig. 7. Hatched region is unstable.

41

Fig. 9.   LF and HF equivalent circuit of junctions coupled in linear array showing LF shunt R_s and HF coupling load Z_L.

Fig. 10.   Power (Δ) and line width ($\square$) as a function of junction number for a low impedance ($\ll 50\ \Omega$) 1-D array of microbridge junctions. $\nu_0 = 10$ GHz, $Z_L = 50\ \Omega$.

Fig. 11.   a) HF equivalent circuit of a junction with a capacitor for perturbation. b) Equivalent circuit as seen by the rest of the array.

Fig. 12.   Relative phases of the oscillators, loop current $\bar{I}_\ell$ and locking current $\bar{I}_{\ell_R}$ for an array of capacitive junctions.

Fig. 13.   Layout of distributed array. Oscillator junctions ($\times$) are placed at wavelength intervals along the serpentine microstrip. Load resistor and detector junction to monitor the load current are shown at upper left.

Fig. 14.   RF current in transmission line (as measured by detector locking range) vs. average frequency junctions in array.

Fig. 15.   a) Micrograph of distributed array. b) Blowup of a), top left, showing detector junction, load resistor and several oscillator junctions on the right. The vertical separation of the oscillators is 10 μm.

Fig. 16.   Power delivered to 23 Ω load resistor vs. array frequency for 40 junction array. Junction parameters $I_c = 2.5$mA, $R = 0.5\ \Omega$.

(a)
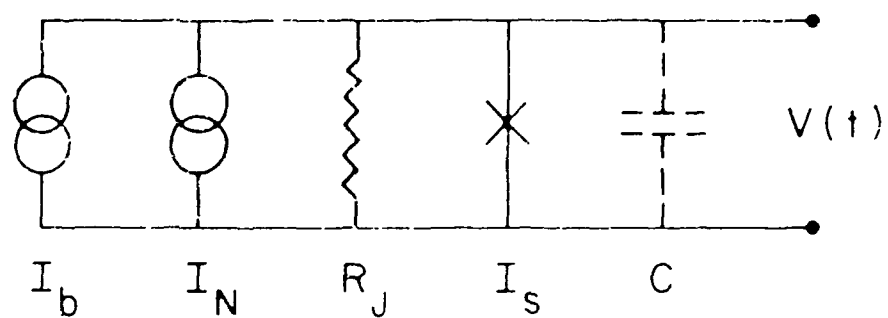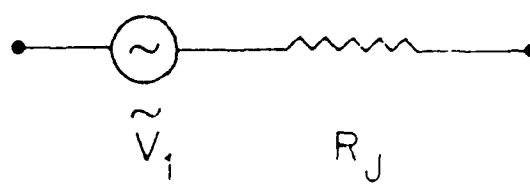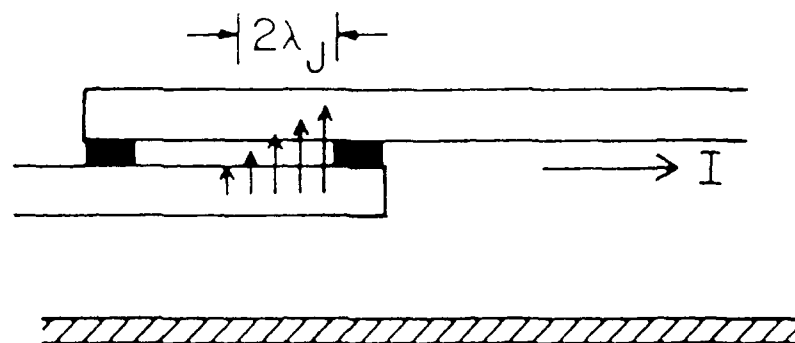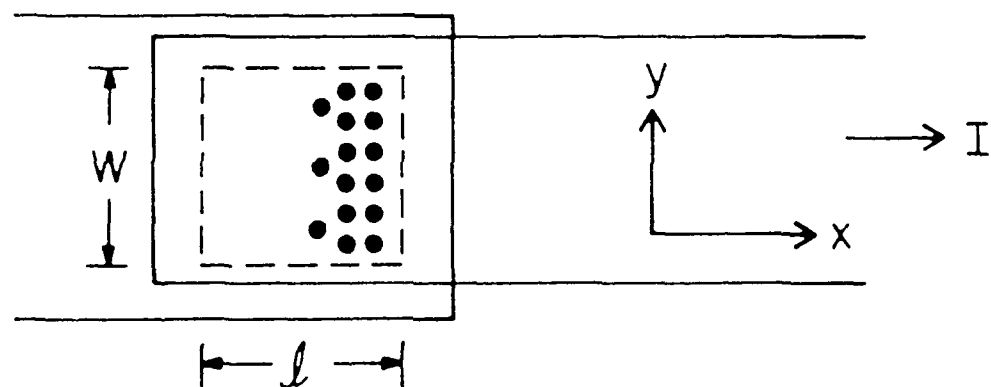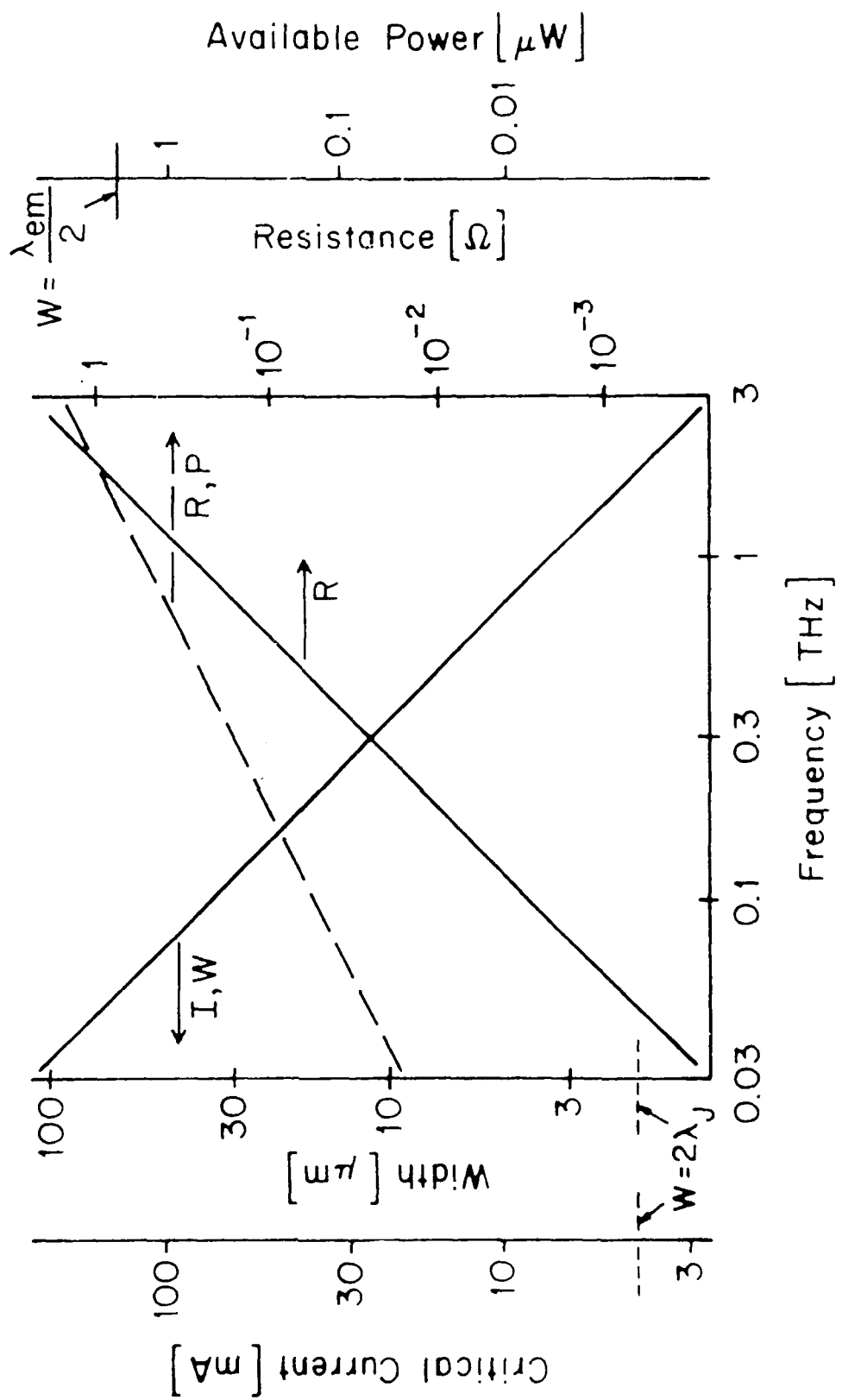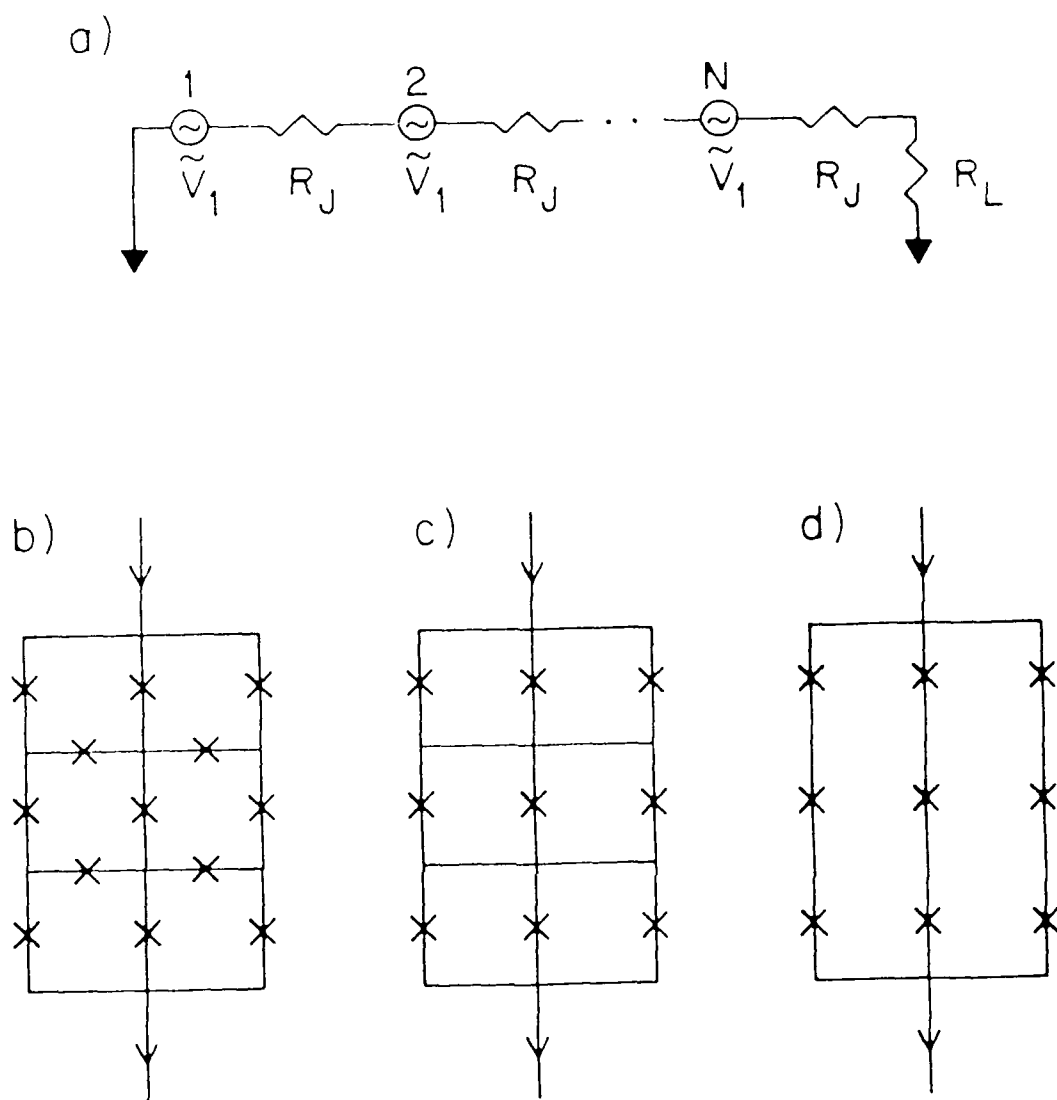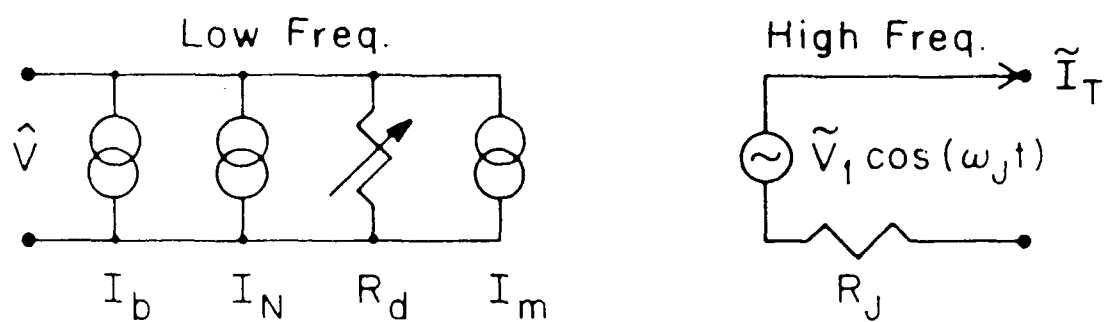
I_b I_N R_J I_S C

(b)

$\tilde{V}_i$ R_J

Fig. 1

(a)

(b)

Fig. 2

44

Fig. 3

45

a)

b)   c)   d)

Fig. 4

Fig. 5

47

Fig. 6

48

Fig. 7

Fig. 8

50

Fig. 9

51

Fig. 10

Fig. 11

53

Fig. 12

Load resistor

Detector junction

Quarter-wave stub

bias lead
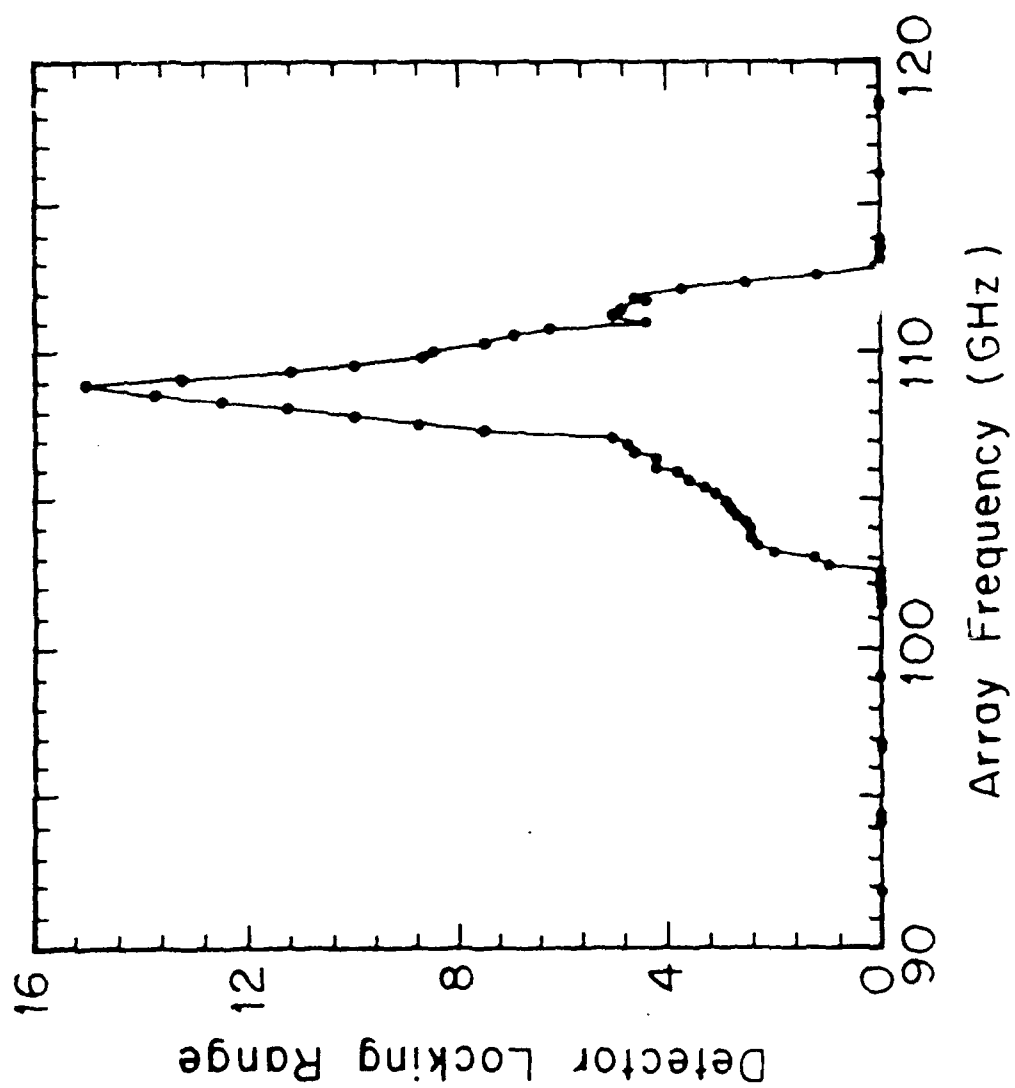
$\dfrac{\lambda}{2}$
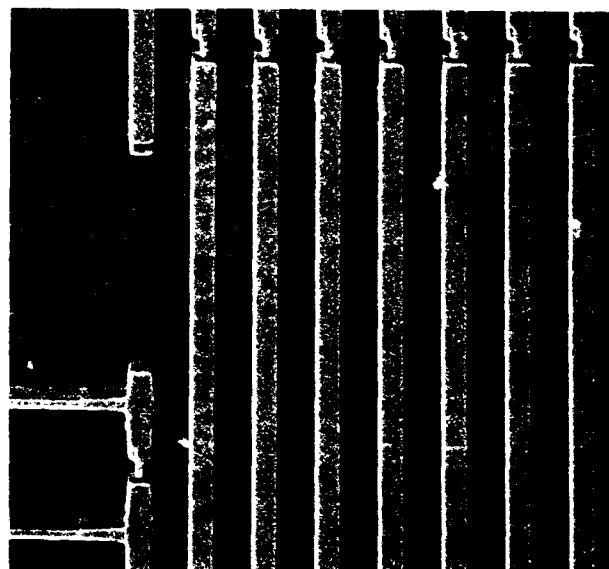
Fig. 13

55

Fig. 14

56
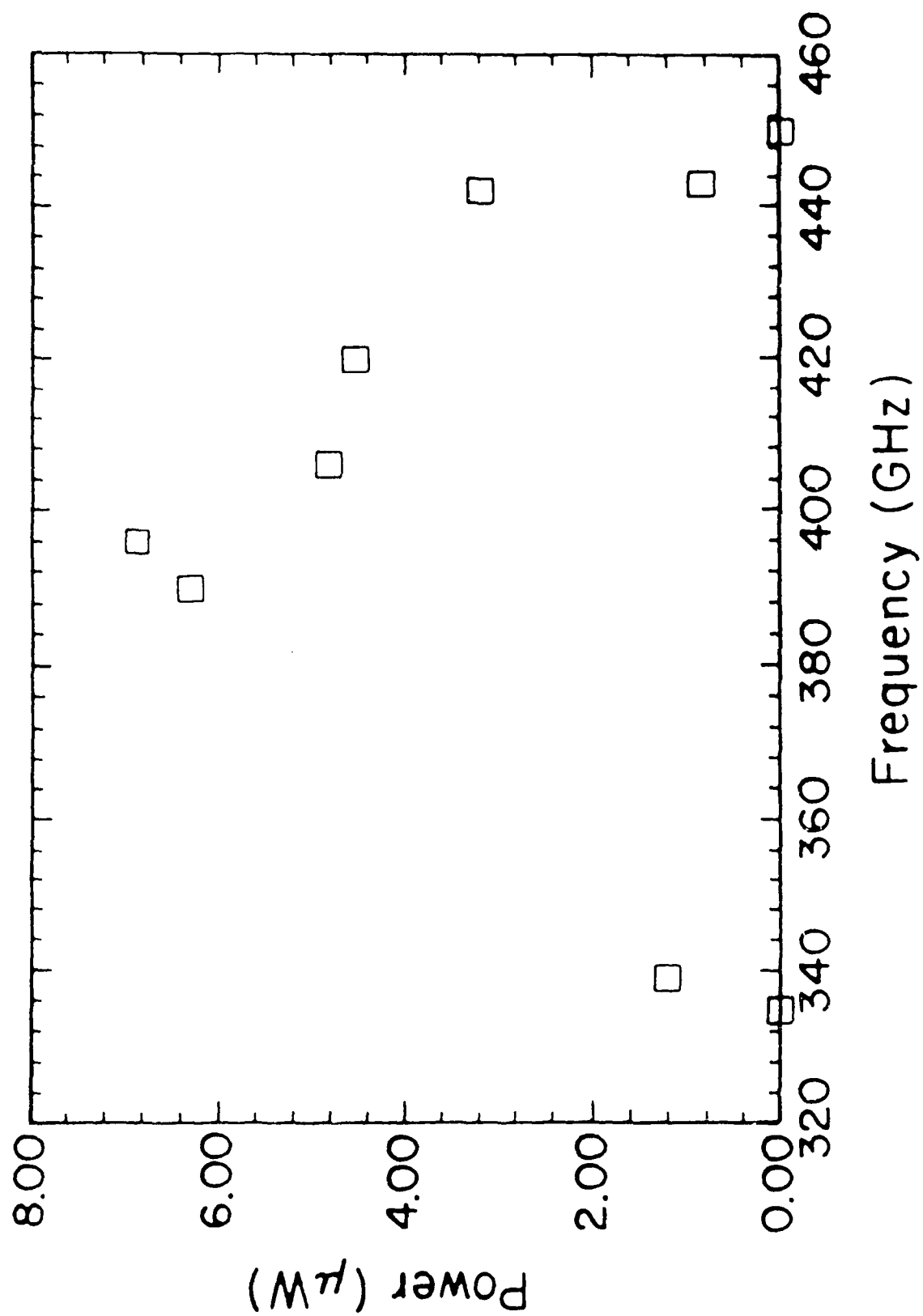
Fig. 15b

Fig. 15a

Fig. 16

58
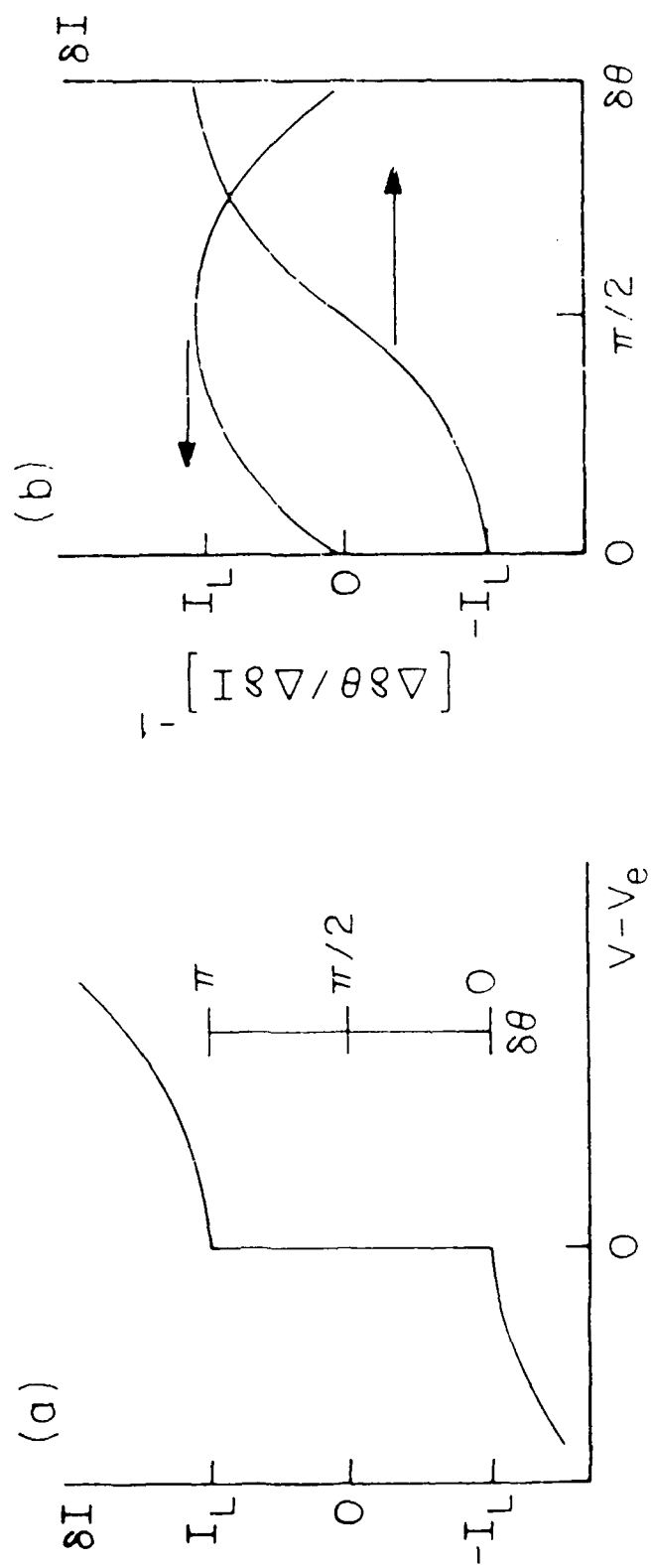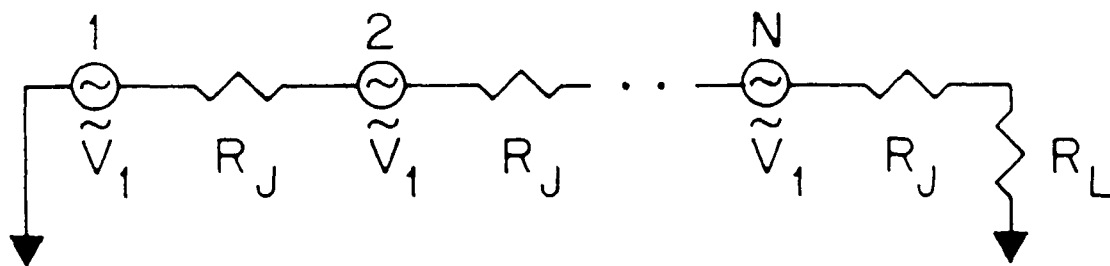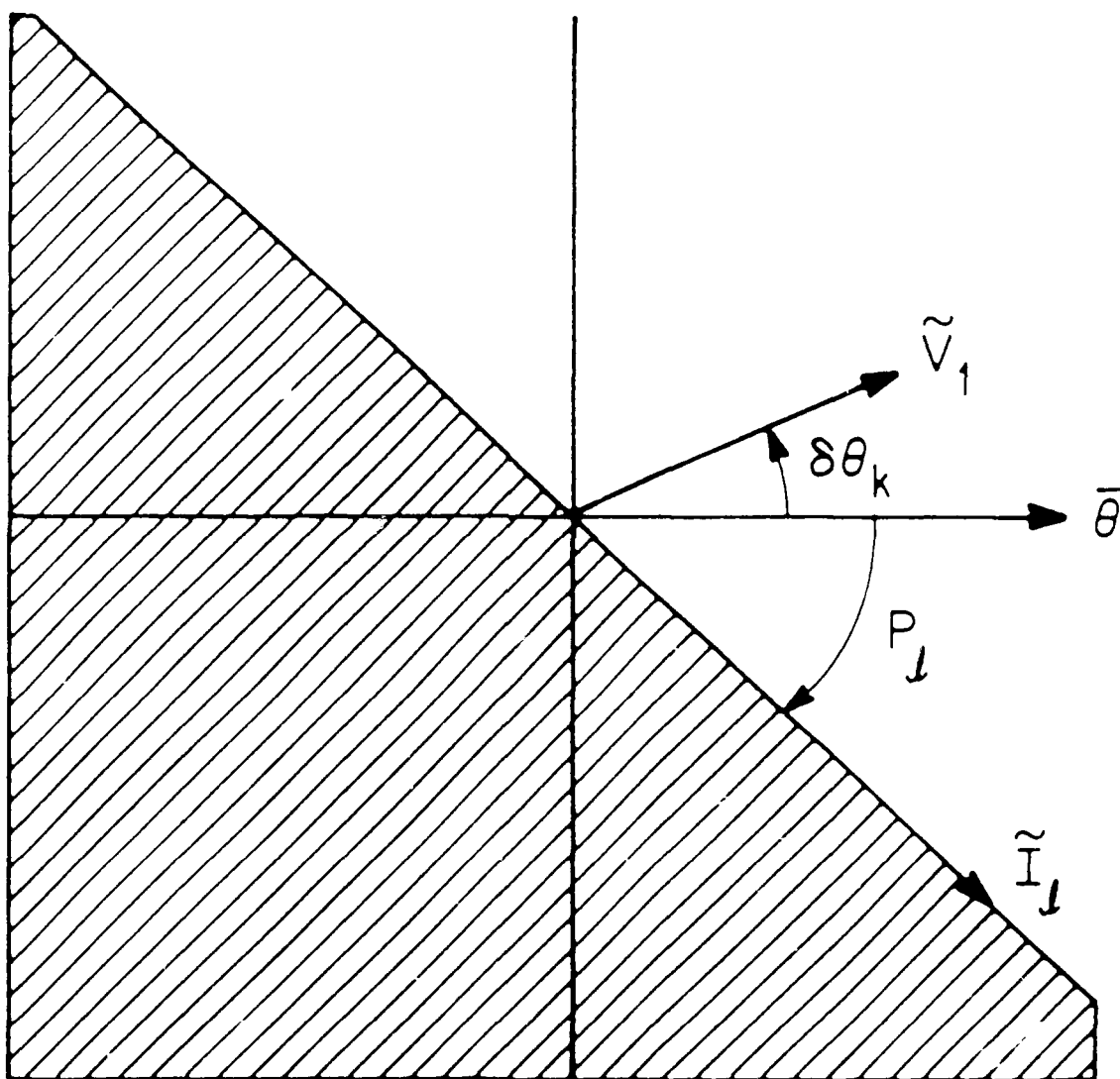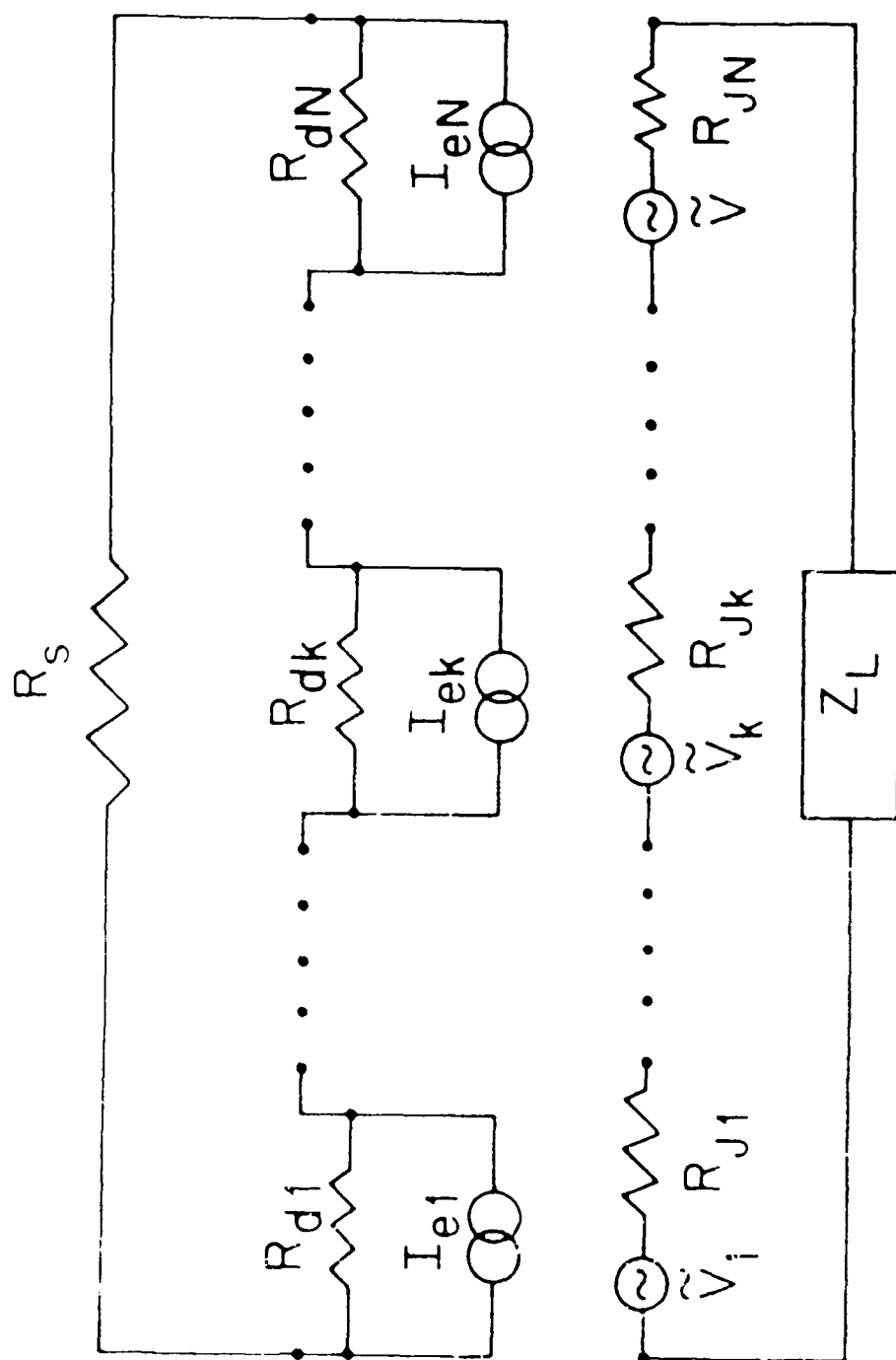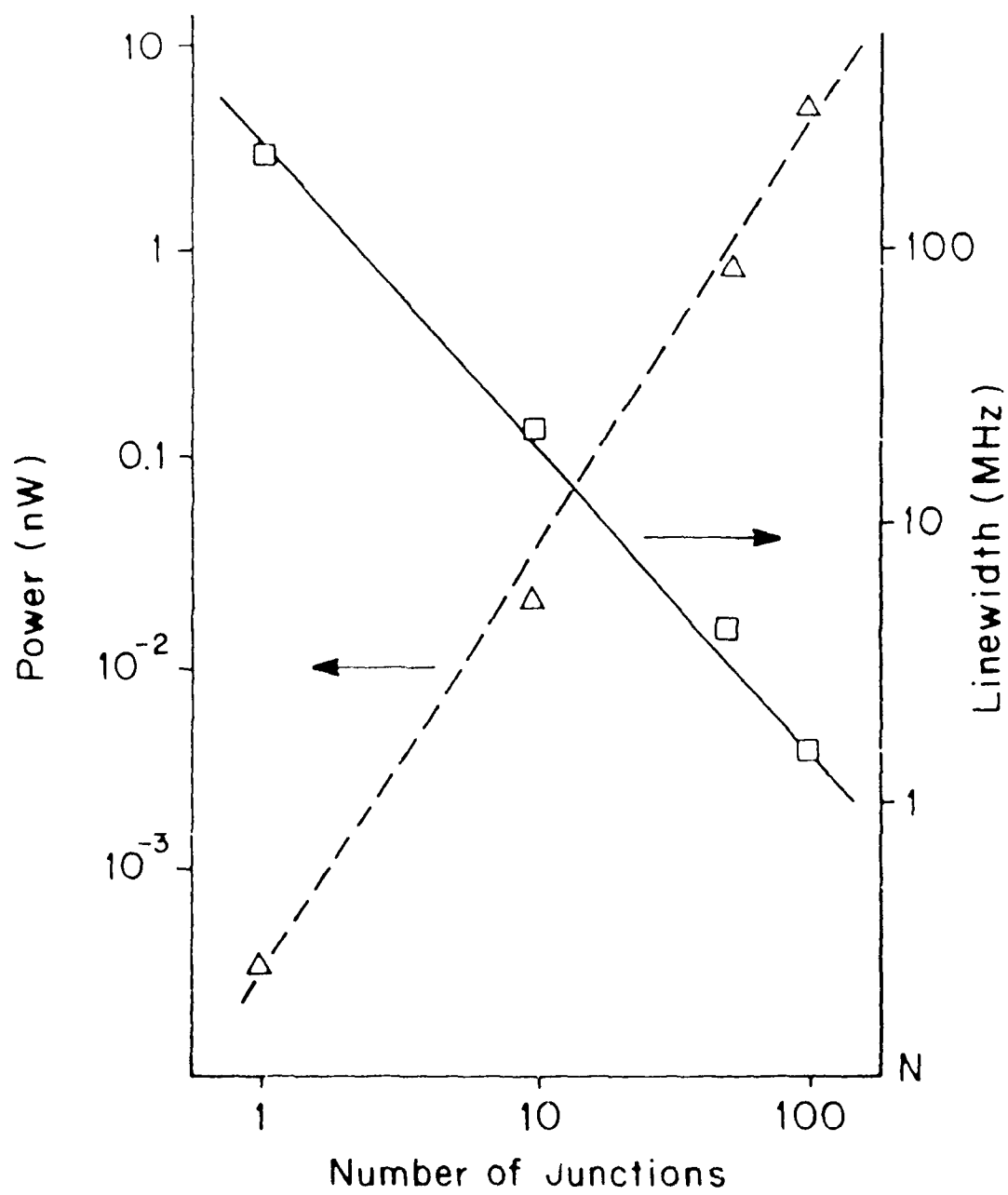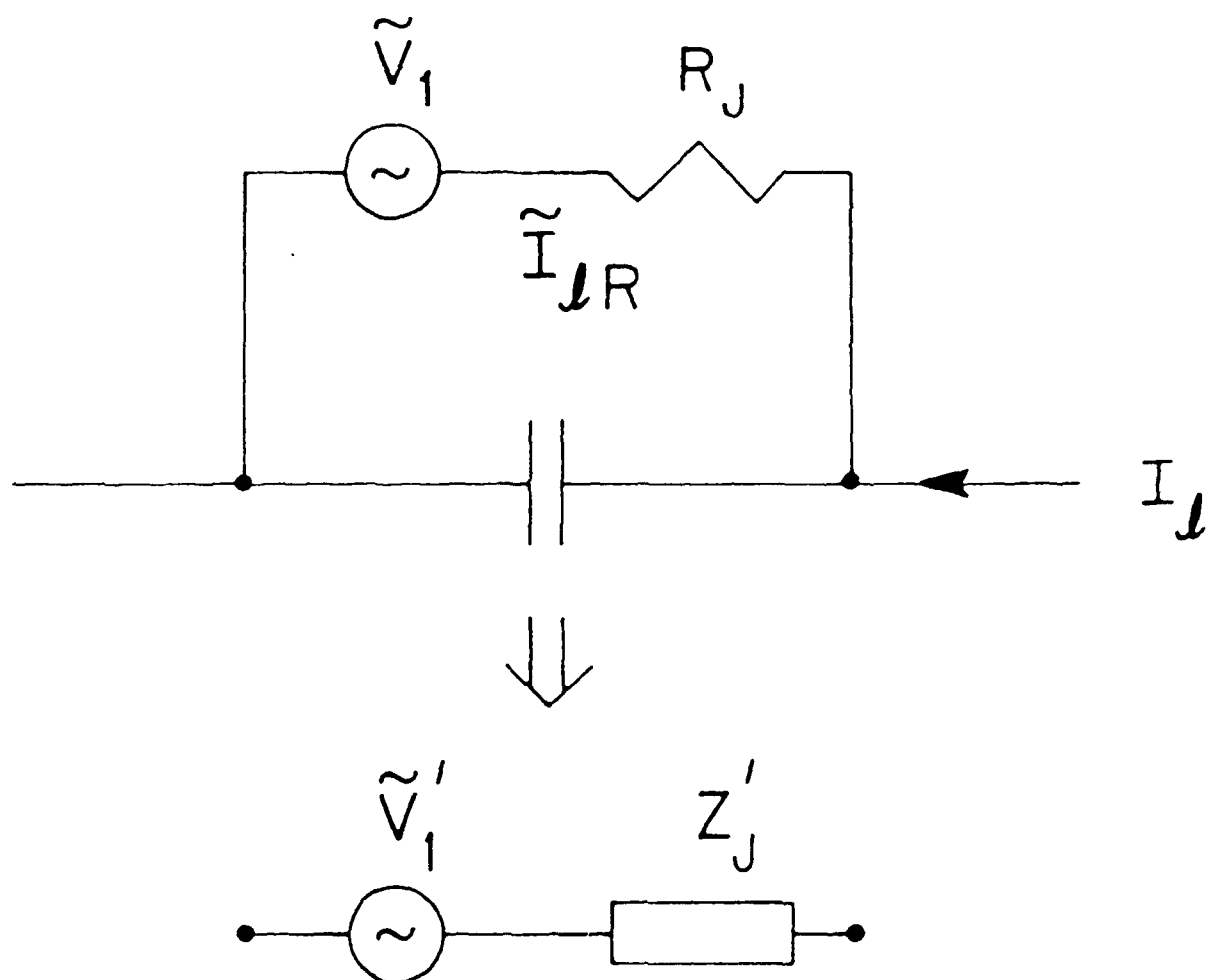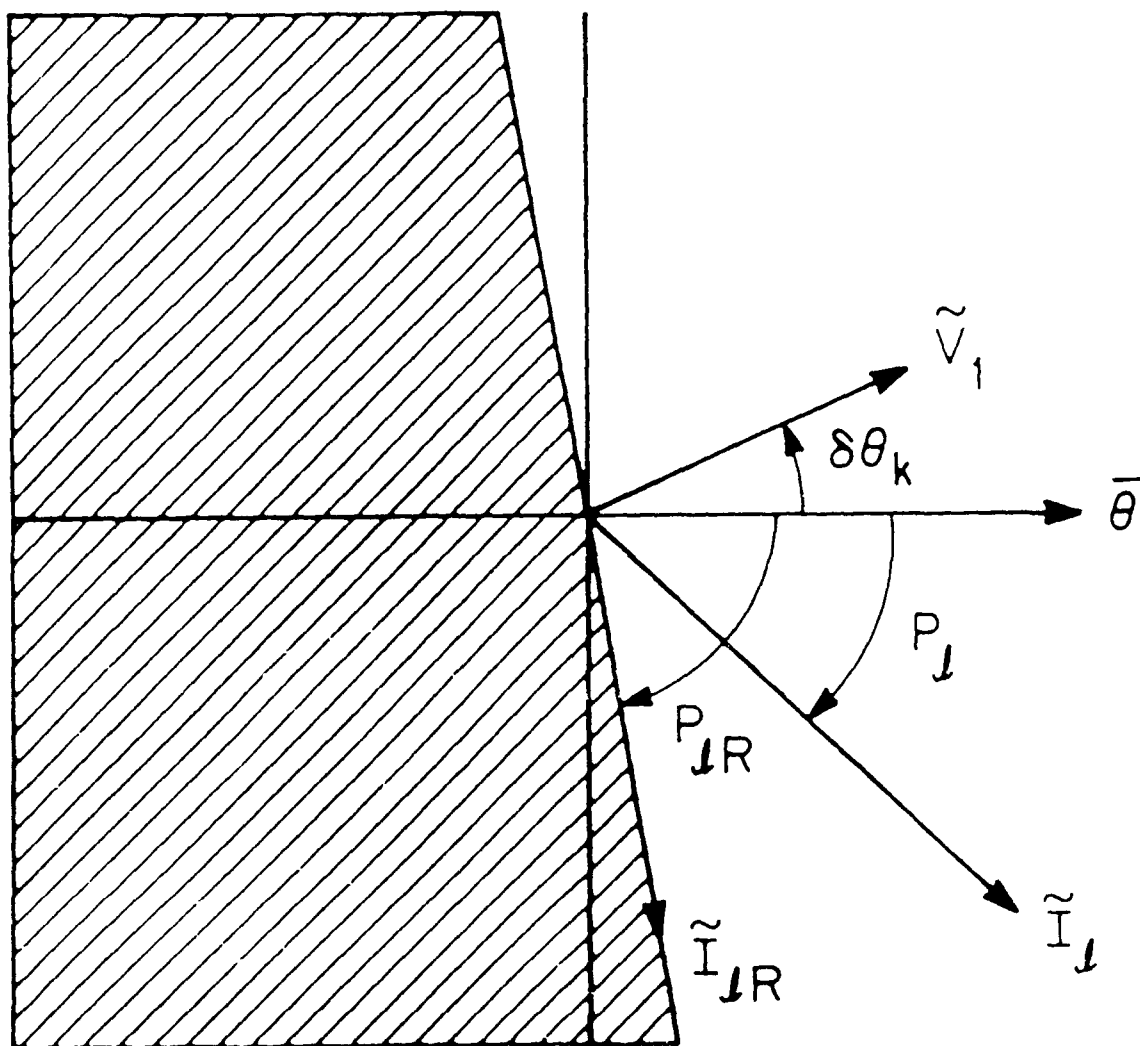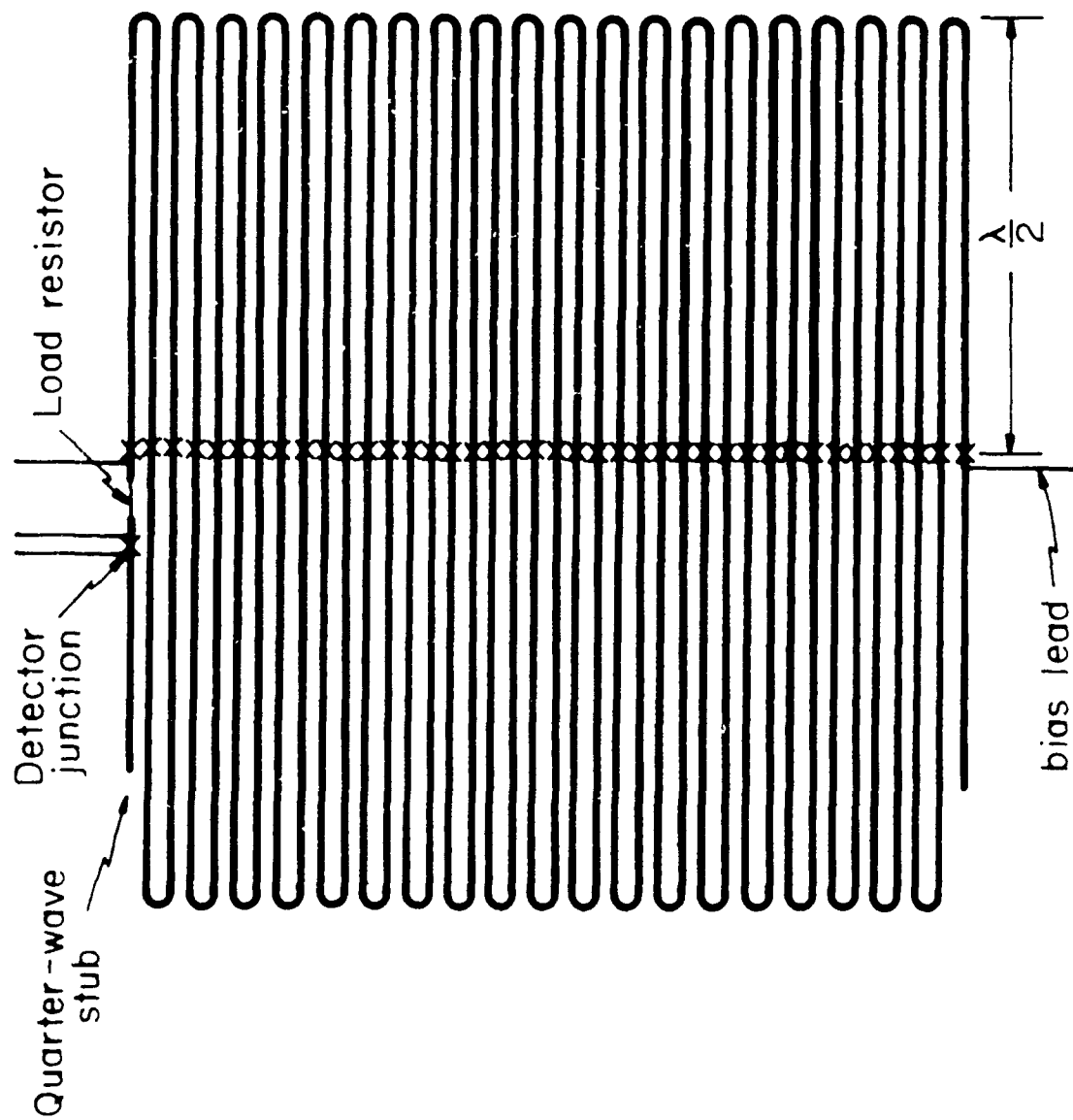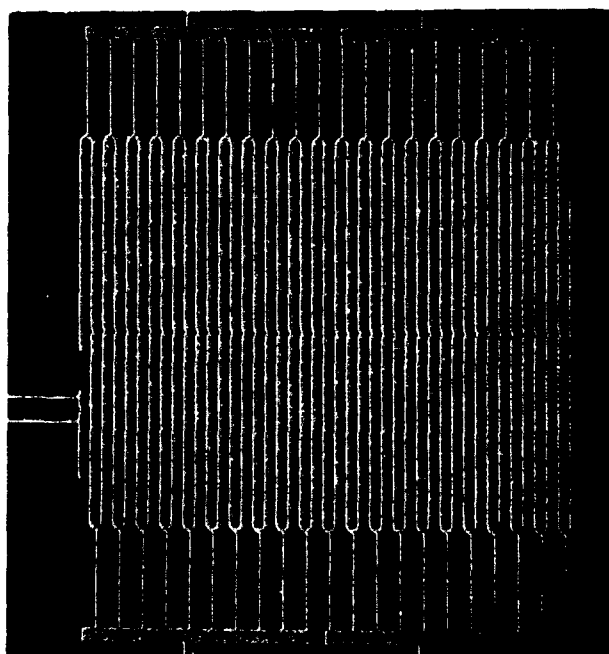
MISSION

of

Rome Air Development Center

RADC plans and executes research, development, test and selected acquisition programs in support of Command, Control, Communications and Intelligence (C^3I) activities. Technical and engineering support within areas of competence is provided to ESD Program Offices (POs) and other ESD elements to perform effective acquisition of C^3I systems. The areas of technical competence include communications, command and control, battle management information processing, surveillance sensors, intelligence data collection and handling, solid state sciences, electromagnetics, and propagation, and electronic reliability/maintainability and compatibility.